Hindawi
Advances in Materials Science and Engineering
Volume 2022, Article ID 2730391, 22 pages
https://doi.org/10.1155/2022/2730391

Research Article

Evaluation of Mechanical and Durability Properties of Eco-Friendly Concrete Containing Silica Fume, Waste Glass Powder, and Ground Granulated Blast Furnace Slag

Mahdi Bameri,[1] **Soroush Rashidi**,[2] **Mohammad Mohammadhasani**,[3] **Mohammad Maghsoudi**,[4] **Hesam Madani**,[5] **and Fereydoun Rahmani**[6]

[1]*Civil Engineering, Tehran, Iran*
[2]*Civil Engineering Structural Engineering, Islamic Azad University Branch of Kerman, Kerman, Iran*
[3]*Seismology Engineering & Risk Department, Building, Housing & Urban Development Research Center (BHRC), Tehran, Iran*
[4]*Department of Civil Engineering, University of Jiroft, Jiroft, Iran*
[5]*Faculty of Civil and Surveying Engineering, Graduate University of Advanced Technology, Kerman, Iran*
[6]*Kerman Cement Industry Group (KCIG), Kerman, Iran*

Correspondence should be addressed to Mahdi Bameri; mahdi.bameri1990@gmail.com

Received 22 April 2022; Revised 21 October 2022; Accepted 26 November 2022; Published 6 December 2022

Academic Editor: Robert Černý

By considering the adverse environmental impacts of the cement manufacturing process, there have been many efforts for cement replacement by supplementary cementitious materials (SCMs), which can enhance the produced concrete performance while reducing cement consumption. This study evaluated the effects of various proportions of silica fume (SF), waste glass powder (WGP), and ground granulated blast furnace slag (GGBFS) on the mechanical and durability properties of concrete. The properties evaluated in this study include compressive, tensile, and flexural strength, magnesium sulfate and sulfuric acid attack, surface resistivity, rapid chloride penetrability test (RCPT), water absorption, depth of penetration of water, and microstructure analysis by scanning electron microscopy (SEM). The results of compressive, tensile, and flexural strength, chloride ion penetrability, and water absorption tests showed that adding 5% of SF to mixtures containing 10% WGP or 10% GGBFS improved concrete performance significantly due to packing density and synergistic effect; however, adding 5% of SF to concrete mixtures decreased the resistance against the magnesium sulfate and sulfuric acid attack. The binary mixture of 15% of WGP showed appropriate performance against the magnesium sulfate and sulfuric acid attack, which may be due to the sacrificial nature of WGP. In addition, the binary mixtures of 15% of WGP and 15% of GGBFS reduced the depth of penetration of water by 45%. Microstructure analysis by SEM showed that the presence of SF, along with WGP and GGBFS, improves the packing density. Finally, adding 5% of SF is suggested to improve the properties of concrete mixtures containing WGP and GGBFS.

1. Introduction

Cement is becoming one of the most widely used worldwide structural materials because of the development of the construction industry. The annual cement production worldwide is reached more than 4.2 billion tonnes and is anticipated to grow continuously [1]. The cement production processes use a large volume of raw materials and energy, and a significant amount of carbon dioxide is released into the atmosphere. According to the type of fuel used, about 0.9–1.0 metric tonnes of CO_2 are released into the atmosphere for every tonne of clinker; if the amount of cement used is reduced, CO_2 emissions will also be reduced [2].

Concrete is the most common construction material in the world, and it is the second most consumed product on the planet after water [3]. Although the concrete industry has destructive effects on the environment and sustainability, it is one of the basic materials for developing the industry, infrastructure, and housing. Portland cement is one of the main components of concrete that reacts with water and produces hydration products through the hydration process. Calcium hydroxide ($Ca(OH)_2$) forms a considerable part of cement hydration products, which is a major drawback in terms of durability. Supplementary cementitious materials (SCMs) reduce the quantity of calcium hydroxide due to the pozzolanic reaction and improve the properties of the concrete which can replace a portion of the cement in the concrete mixture. SCMs are from industrial byproducts or natural materials; these materials react with hydrated cement paste both hydraulically or pozzolanic, which can lead to the production of durable and economical concretes [4–8]. Engineering, economic, and ecological advantages can be achieved by replacing a portion of cement with SCMs. The engineering advantage can be attributed to the improvement potential of the fresh and hardened concrete properties by adding an appropriate portion of SCMs, such as silica fume, to the concrete mixture [9]. Moreover, replacing some amount of the cement with cheaper options, such as waste glass powder and ground granulated blast furnace slag (GGBFS), can also obtain economic advantages [10–12]. Also, due to the consumption of less cement in the concrete mixture, environmental pollution can be prevented by reducing CO_2 emissions [13].

For decades, the focus has been fully developed on SCMs. Many studies have been carried out on their utilization in concrete production and evaluating their effects on hardened concrete properties [14–16]. SCMs are considered options for Portland cement in the concrete mixture for economic and ecological reasons, improving the mechanical and durability properties and minimizing the penetrability of concrete. Nevertheless, few studies have been carried out on industrial byproducts with cementitious or pozzolanic properties as replacements for cement [17].

Studies have demonstrated that pozzolanic materials have a significant amount of amorphous silica (silicon dioxide) in their chemical composition [17, 18]. By adding pozzolanic materials to the concrete mix proportion, a reaction takes place between silicon dioxide (SiO_2) and $Ca(OH)_2$, which is called the pozzolanic reaction [19]. The cement hydration process produces $Ca(OH)_2$, and it causes adverse effects on concrete durability due to higher solubility in acids and sulfates compared to other products. The affection of SCMs in the pozzolanic reaction and the $Ca(OH)_2$ conversion to calcium silicate hydrate (C-S-H) leads to an increase in the durability of the concrete exposed to the penetration of acids, sulfates, and chloride ions, also increasing the concrete density [21]. The main advantages of SCMs are attributed to the three properties of the pozzolanic reaction. First, the rate of reaction is reduced, which leads to a decreased heat of hydration and reduces the rate of strength development of concrete [19]. Second, the SCMs' reaction with $Ca(OH)_2$ leads to a decreased amount of this unfavorable product in the concrete, which significantly affects its durability and penetrability [21–23]. Third, they reduce the capillary pores, increasing the concrete impermeability and strength [24]. Nonetheless, the use of SCMs has limitations. That is, the reactivity of SCMs is generally lower than cement [25, 26].

Investigations show that the worldwide production of GGBFS is 300–360 million tonnes annually, so only part of the demand for cement can be fulfilled by replacing GGBFS [25, 27, 28]. Accordingly, the focus of many researchers is the identification of alternative SCMs and the evaluation of their performance in concrete.

The waste glass powder is one of the widely available materials that can be utilized as a replacement for cement. A small amount of waste glass is recycled, and the remainder of it is disposed of due to impurities available in it or color or cost. Due to the different properties of waste glass powder, recycling any type of waste glass is impossible. There is a need to create new options for recycling waste glass. One important option is to use waste glass in building materials [25, 29]. The glass powder contains 73% SiO_2, 13% Na_2O, and 10% CaO, making it a pozzolanic material, and can be utilized in concrete [25, 30]. In 1963, the first study on the usage of glass for building materials was done. The authors used waste glass aggregates to produce a wall panel [31]. Later, due to the hardness of glass, many studies were conducted to use waste glass as aggregate in concrete and mortar [32–34]. Since glass has alkali content, replacing glass as aggregate in concrete is vulnerable to the alkali-silica reaction. The performance of concrete and the alkali-silica reaction depends on the size of the glass particles. The alkali-silica reaction in concrete can be reduced by adding silica fume, GGBFS, fly ash, and metakaolin [25]. Utilizing glass powder as SCM in the studies of Islam et al. [35], He et al. [36], Patel et al. [37], Mehta and Ashish [25], and Ibrahim [38] was investigated [25, 35–38]. According to the literature reviewed, 10–20 wt% of waste glass powder can be utilized as a replacement for cement. Mehta and Ashish [25] evaluated the effects of silica fume and waste glass on the workability, strength, durability properties, and microstructural analysis of concrete. They remarked that the optimal replacement percentage of glass powder by cement is 10%, which can significantly improve concrete performance [25].

The SCMs have low rates of lime consumption at early ages [39, 40]. Although improving the mechanical and durability properties of concrete in the long term, these materials could not improve the mechanical and durability properties of concrete in the short term [41]. Among SCMs, fly ash and GGBFS are the most common types that have been utilized at high replacement levels. However, silica fume and metakaolin cannot be added to the concrete at a high replacement level because these materials significantly reduce the workability of concrete due to the very high surface area [41, 42]. The pozzolanic properties of silica fume and its filling effect have made it an appropriate SCM [25, 43]. Adding silica fume to concrete can reduce bleeding, porosity, and penetrability [44]. The fine particle size of silica fume allows it to act as a filler and improve the packing density by being placed among the cement particles [41, 45].

According to the advantages and disadvantages of GGBFS, the above-mentioned waste glass powder and silica fume may have synergistic effects to improve concrete properties. Although silica fume can improve the cement hydration and durability characteristics of concrete, it reduces the workability of concrete, and adding high amounts of silica fume in concrete is not applicable. Hence, combining silica fume with low surface area SCMs such as glass powder and GGBFS can increase the workability (flowability) of concrete, so ternary concrete mixtures can be an effective solution to utilizing higher volumes of SCMs in sustainable concrete. Although the low reactivity of GGBFS and glass powder due to their particle size reduces the strength of concrete at early ages, silica fume increases the strength of concrete because of its finer and more reactive particles. In ternary concrete mixtures, adding silica fume improves the density as they fill the spaces between the cement, GGBFS, and glass powder particles, reducing the number of voids in the packing and consequently increasing the packing density. Furthermore, the risk of alkali-silica reaction of concrete containing glass powder can be reduced by adding silica fume. The ternary concrete mixtures can exhibit acceptable durability and strength performances at different ages and decrease vulnerability under aggressive environmental conditions; consequently, using ternary mixtures can be an appropriate option [25, 41].

Several studies have been conducted on the properties of ternary concrete mixtures containing silica fume. Yazıcı [46], Bagheri et al. [47], and Wongkeo et al. [48] stated that ternary concrete mixtures containing fly ash and silica fume increased chloride resistance compared to binary concrete mixtures containing fly ash without silica fume [46–48]. Wongkeo et al. [48] and Li and Kwan [49] reported that the addition of silica fume to concrete mixtures containing fly ash might improve the mechanical properties of concrete [48, 49]. Ibrahim [38] reported the results of three groups of mixture designs, including plain concrete, concrete containing silica fume, and concrete containing fly ash. The cement content was replaced by 5%, 10%, 15%, and 20% waste glass powder. The results showed that 5% of waste glass powder could replace cement without reducing the compressive and tensile strength. In addition, replacing 20% of waste glass powder in concrete containing silica fume and fly ash reduced the compressive and tensile strength by 13–14%, respectively [38].

Regarding sustainable development, the current study evaluated the effect of GGBFS and waste glass powder with/without silica fume on the mechanical and durability properties of eco-friendly concrete. To accurately evaluate the synergistic effects of concrete mixtures, tests of compressive strength, tensile strength, flexural strength, magnesium sulfate attack, sulfuric acid attack, surface resistivity, rapid chloride penetrability test (RCPT), water absorption, depth of penetration of water, and microstructure analysis of concrete by SEM were performed.

2. Materials and Methods

2.1. Materials

2.1.1. Supplementary Cementitious Materials (SCMs). Ordinary Portland Cement (OPC)-Type II [50], produced by Kerman Momtazan Cement Co., (KMCC) in Iran, Kerman, and three types of SCMs, including silica fume (SF), ground granulated blast furnace slag (GGBFS), and waste glass powder (WGP), were used in this study for concrete production. Iran Ferrosilice Co., Esfahan Steel Co., and Baztab Rah Co., supply SF, GGBFS, and WGP are used in the current study, respectively. The chemical, physical, and mechanical properties of the intended materials are demonstrated in Table 1.

SF added in concrete mixtures is characterized by light grey color and is composed of at least 85% SiO_2 based on ASTM C1240 [51]. According to ASTM C989, the activity index of GGBFS lies between grades 80 and 100 [52]. WGP consists of 71% SiO_2, 3.2% Al_2O_3, and 0.19% Fe_2O_3, and it can be treated as pozzolanic material concerning chemical requirements presented in ASTM C618 despite the alkali content [53]. The laser particle size analyzer (LPSA) is employed to determine the particle size distribution of cement and other SCMs, as shown in Figure 1. It must be noted that the particle size distribution of the SF in Figure 1 shows the size of agglomerates and does not show the particle size [43].

2.1.2. Aggregates. The aggregates used in this study include natural sand with a maximum nominal size of 4.75 mm, saturated surface dry (SSD) density of 2630 kg/m^3 and SSD water absorption of 2.07%, and coarse aggregate with a nominal maximum size of 19 mm, SSD density of 2690 kg/m^3, and SSD water absorption of 0.9% [54, 55]. It is to be noted that the gradation of the used aggregates meets the requirements of ASTM C33 [56]. Mechanical sieve shakers are used to determine the size distribution of aggregates, and analysis results can be seen in Figure 2.

2.1.3. Superplasticizer. The polycarboxylate ether-based superplasticizer (PES) with a specific gravity of 1.1 g/cm^3 and *pH* value of 6.2 was added to all concrete mixtures according to ASTM C494 [57].

2.2. Mix Proportions.

In this experimental study to evaluate the mechanical and durability properties of concrete, six mixture proportions with SCMs described in the previous section were considered. The binder content and water/binder ratio were kept constant in all the mixtures at 400 kg/m^3 and 0.36, respectively. The concrete mixture proportions are presented in Table 2.

2.2.1. Production Method and Curing Conditions for Concrete Mixtures. Materials were mixed in the following order. First, coarse aggregate and a half of sand were drily mixed for 1 min; then, the rest of the sand, cement, SCMs, and 2/3 of mixing water was added, and the mixing process was resumed for 3 min further; finally, the rest of the water along with the superplasticizer was also added and was mixed for another 8 min. After 24 h casting, all the specimens were demolded, and according to BS EN

Table 1: Chemical, physical, and mechanical properties of cement, SF, GGBFS, and WGP.

Properties	Cement (%)	SF (%)	GGBFS (%)	WGP (%)
Silicon dioxide (SiO_2)	21.13	Min 85.00	36.50	71.00
Aluminium oxide (Al_2O_3)	4.55	Max 1.00	11.00	3.23
Ferrous oxide (Fe_2O_3)	3.63	Max 2.00	0.70	0.19
Calcium oxide (CaO)	63.72	Max 1.50	38.50	9.20
Magnesium oxide (MgO)	1.27	Max 1.50	9.20	1.49
Sulphur tri oxide (SO_3)	2.58	—	0.30	0.19
Insoluble residue (IR)	0.49	—	0.40	100.00
Sodium oxide (Na_2O)	0.16	—	0.55	13.80
Potassium oxide (K_2O)	0.59	—	0.60	0.29
Loss on ignition (LOI)	1.67	Max 3.50	0.50	0.67
Tricalcium silicate (C_3S)	55.71	—	—	—
Dicalcium silicate (C_2S)	18.61	—	—	—
Tricalcium aluminate (C_3A)	5.92	—	—	—
Tetra-calcium aluminoferrite (C_4AF)	11.01	—	—	—
Physical properties				
Median diameter (D50) (μm)	21	4*	16	30
Specification surface (cm^2/gr)	3110	150,000–200,0000	4000	2900
Soundness: Autoclave expansion, (%)	0.11	—	—	—
Soundness: Le Chatelier expansion, (mm)	1.00	—	—	—
Setting time (min)	Initial-135	—	—	—
	Final-185	—	—	—
Mechanical properties				
Mortar compressive strength (MPa)				
3 days	27.6	—	—	—
7 days	36.3	—	—	—
28 days	47.3	—	—	—

*Median diameter of agglomerated silica fume.

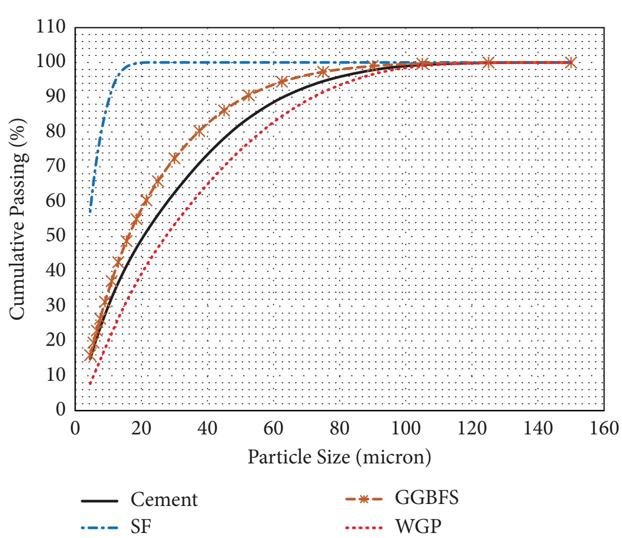

Figure 1: The particle size distribution of cement, SF, GGBFS, and WGP.

12390-2, they were cured in water at $20 \pm 2^{\circ}C$ until the time of testing [58].

2.3. Test Methods

2.3.1. Compressive Strength. According to BS EN 12390-3, the compressive strength tests were carried out on cubic specimens with dimensions of $150 \times 150 \times 150$ mm at the ages of 7, 28, 56, and 90 days [59].

2.3.2. Tensile Strength. According to ASTM C496, the tensile strength tests were carried out on cylindrical specimens with a diameter of 150 mm and a height of 300 mm at the ages of 7, 28, 56, and 90 days. The loading rate was 103 kg/s [60].

2.3.3. Flexural Strength. According to ASTM C293, the flexural strength tests were carried out on beam specimens with dimensions of $100 \times 100 \times 500$ mm at the ages of 7, 28, 56, and 90 days [61].

2.3.4. Magnesium Sulfate and Sulfuric Acid Attack. The magnesium sulfate attack tests were performed at the ages of 7, 28, 56, and 90 days. This test method evaluates the chemical resistance of concrete under anticipated service conditions for which 1.5% magnesium sulfate was used to stimulate the magnesium sulfate environment. The magnesium sulfate solution pH was kept in the range from 5 to 7 by adding sulfuric acid throughout the test duration. Oven-dried concrete cubes ($150 \times 150 \times 150$ mm) were weighed first and then completely submerged in the magnesium sulfate solution. Three cubes of each mixture were tested after each exposure period. Weight change was compared with the initially measured weight. Compressive strength changes of concrete specimens exposed to magnesium sulfate were also performed at mentioned ages. Finally, these results were compared with the compressive strength of 28 days of water-cured concrete specimens. The sulfuric acid

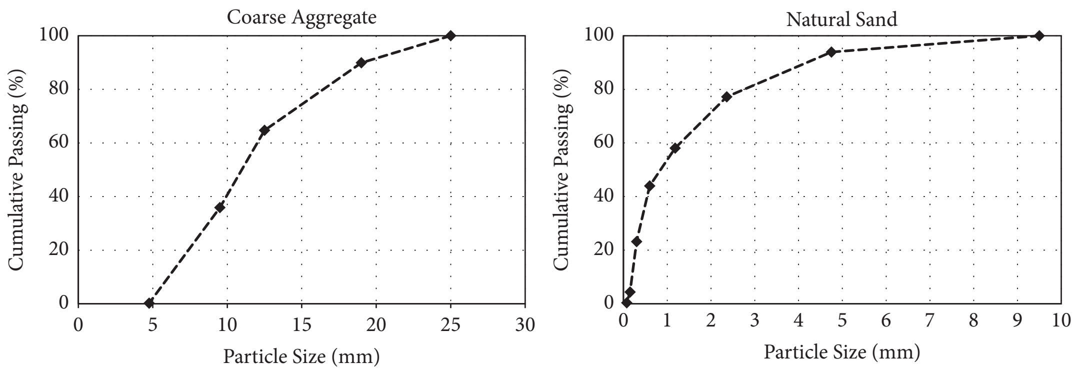

Figure 2: Particle size distribution curves of aggregates.

Table 2: Proportions of the concrete mixtures.

Mix	Mix code	W/B	Unit content (kg/m^3)						
			Water	Cement	SF	WGP	GGBFS	Natural sand	Coarse aggregate
Control	Ctrl	0.36	144	400	—	—	—	930	907
SF (5%)	SF5	0.36	144	380	20	—	—	925.2	902.1
WGP (15%)	WGP15	0.36	144	340	—	60	—	923.8	900.6
GGBFS (15%)	GGBFS15	0.36	144	340	—	—	60	933.2	910.3
SF (5%) + WGP (10%)	SF5+WGP10	0.36	144	340	20	40	—	921.1	897.9
SF (5%) + GGBFS (10%)	SF5+GGBFS10	0.36	144	340	20	—	40	927.4	904

SF: silica fume, GGBFS: ground granulated blast furnace slag, and WGP: waste glass powder.

attack tests were also performed in a similar method with the only difference that the *pH* value was equal to 1.0 [62–72].

2.3.5. Surface Resistivity. According to AASHTO-T 358, the surface resistivity was measured in kΩ·cm by placing the four-point Wenner array probe on cylindrical specimens with dimensions of 100 × 200 mm [73].

2.3.6. Rapid Chloride Penetrability Test (RCPT). As seen in Figure 3, the RCPT was performed according to ASTM C1202. At the age of 28, 56, 90, and 120 days, three 50 mm thick slices were cut from the middle part of 100 × 200 mm cylindrical specimens of each mixture. Finally, direct current (DC) by a constant 60-volt potential difference was applied to them for 6 hours [74].

Figure 3: Rapid chloride penetrability test (RCPT).

2.3.7. Water Absorption. According to BS 1881-122, the water absorption tests were carried out on cubic specimens of dimensions 100 × 100 × 100 mm at the ages of 28, 56, 90, and 120 days. The specimens were removed from the water and subsequently were dried at 105°C for 72 h in an oven until they reached a constant weight. The weighted specimens were then immersed in the water for 30 minutes and 24 hours. The amount of water absorbed by each specimen was determined by weighting each specimen again [75].

2.3.8. Depth of Penetration of Water under Pressure. As can be observed from Figure 4, this test is carried out according to BS EN 12390–8 to measure the depth of penetration of water in cubic specimens of dimensions 150 × 150 × 150 mm under 500 kPa pressure during 72 h [76].

2.3.9. Scanning Electron Microscopy (SEM). The SEM allows the chemical analysis and examination of the composition, surface, and concrete microstructure at the micro- and nano-scale. In the current study, SEM of voltage 10 kV and magnification 10.0000x examined the microstructure of concrete specimens. The concrete specimens of tests had the age of 90 days with dimensions of 10 × 10 × 10 mm, and a gold layer coated them before analysis.

3. Test Results and Discussion

3.1. Mechanical Tests

3.1.1. Compressive Strength. The compressive strength test usually provides an overview of concrete quality because the compressive strength of concrete is directly related to

Figure 4: Depth of penetration test of water under pressure.

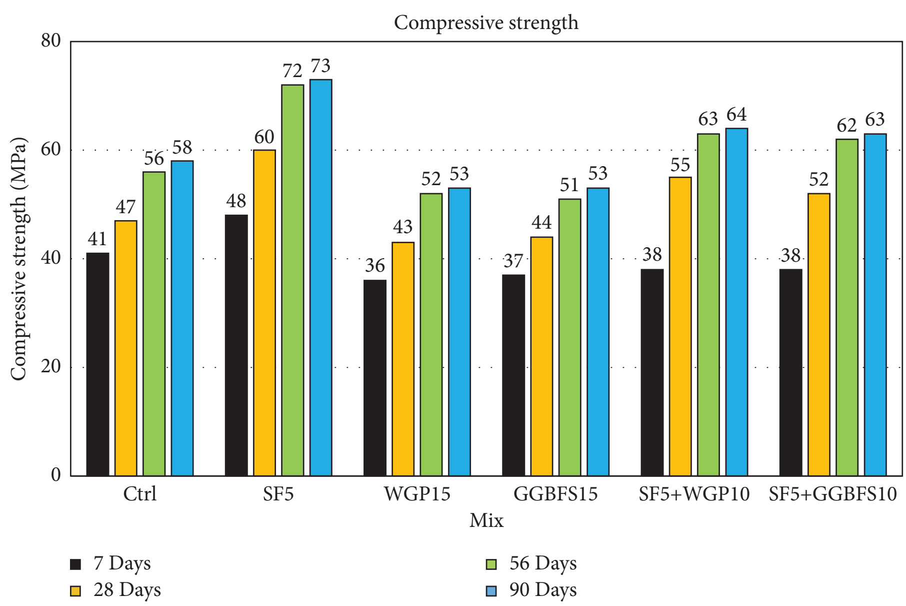

Figure 5: Compressive strength results of concrete mixtures.

the structure of the hydrated cement paste [38]. Figure 5 shows the results of compressive strength. According to that, the highest compressive strength is related to the binary specimen of SF5 because compared to the Ctrl specimen, at the ages of 7, 28, 56, and 90 days, 17%, 27.6%, 28.5%, and 25.8% increased compressive strength, respectively. SF particles with an average diameter of 150 nm are significantly smaller than cement particles with an average diameter of 15 μm, so they can fill the pores and improve the characteristics of concrete; this is known as particle packing or space-filling. In addition, the pozzolanic reaction of SF with $Ca(OH)_2$ in cement paste causes the formation of C-S-H, which fills the interfacial transition zone (ITZ) and improves compressive strength [41, 43, 77–85].

In the ternary specimens of SF5 + WGP10 and SF5 + GGBFS10, at the age of 7 days, a 7.3% reduction in compressive strength compared to the Ctrl specimen can be seen; the reason is the slow rate of pozzolanic reactions of WGP and GGBFS at early ages [86–88]. But, at the ages of 28, 56, and 90 days, the ternary specimen of SF5+WGP10 obtained 17%, 12.5%, and 10.3% increases in compressive strength, respectively, compared to the Ctrl specimen because the dissolution of glass particles leads to the creation of free alkali Na^+ and Si^+ ions [89, 90]. Na^+ and Si^+ released from glass powder and hydroxyl ions from cement hydration maintain the *pH* of the pore solution between 13 and 14. The high *pH* of the pore solution increases the solubility of amorphous silicates [91]. Therefore, the rate of the SF reaction increases, and as a result, denser C-S-H is formed.

Also, at the ages of 28, 56, and 90 days, the ternary specimen of SF5 + GGBFS10 obtained 10.6%, 10.7%, and 8.6% increase in compressive strength compared to the Ctrl specimen, respectively. The increase in compressive strength is due to very fine and reactive particles of SF. The C-S-H gel is produced during the reaction with the SF adsorbed on the GGBFS surface; as a result, the unreacted GGBFS particles connect with the gel around it tightly. The unreacted GGBFS particles are also tightly connected to the surrounding $Ca(OH)_2$ crystals due to the reaction between the $Ca(OH)_2$ crystal and the SF adsorbed on the GGBFS surface [87]. Generally, the presence of SF, along with WGP and GGBFS, provides a sufficient amount of silica, sodium, and calcium to react with $Ca(OH)_2$ and accelerate the rate of C-S-H formation [92]. In truth, the increases in compressive strength in SF5 + WGP10 and SF5 + GGBFS10 specimens indicate the synergistic effect of ternary mixtures [93].

In the binary specimen of WGP15, a decrease in compressive strength was observed at all ages compared to the Ctrl specimen. The reduction in compressive strength at the ages of 7, 28, 56, and 90 days was 12.2%, 8.5%, 7.1%, and 8.6%, respectively. Ibrahim [38] and Aliabdo et al. [94] confirmed these results; they stated that at WGP15%, the compressive strength decreased [38, 94]. In truth, the pozzolanic reaction of glass powder is directly related to its particle size. Finer particle size produces a higher pozzolanic reaction. Therefore, the strength increase rate is affected by the particle size distribution of the glass powder [95].

The compressive strength results in the binary specimen of GGBFS15 are similar to the binary specimen of WGP15. The hydration activity of GGBFS is significantly lower than that of cement at early ages. Moreover, GGBFS has a retarding effect on cement hydration at early ages [87]. Therefore, the initial compressive strength of concrete containing GGBFS is significantly lower than that of plain concrete [96].

3.1.2. Splitting Tensile Strength. Figure 6 shows the tensile strength test results of cylindrical concrete at the ages of 7, 28, 56, and 90 days. Similar to the compressive strength results, the highest tensile strength is related to the binary specimen of SF5 because, at the ages of 7, 28, 56, and 90 days, 19.4%, 13%, 27.6%, and 16.9% of strength increased, compared to the Ctrl specimen, respectively. SF particles are 100 times smaller than cement particles, so they can be well placed among the cement particles and cause more densification in the cement paste matrix. In addition, the pozzolanic reaction of SF with $Ca(OH)_2$ induces the formation of C-S-H. Hence, the compact microstructure of the cement paste, especially in the ITZ, leads to an increase in tensile strength [78, 97].

In the ternary specimens of SF5 + WGP10 and SF5 + GGBFS10 at the age of 7 days, 30.5% and 33.3% reduction in tensile strength was observed compared to the Ctrl specimen, respectively. The reason for this is the slow reactivity of WGP and GGBFS at early ages to cement [86–88]. Nevertheless, at the ages of 28, 56, and 90 days, the ternary specimen of SF5 + WGP10 obtained 8.7%, 23.4%, and 11.3% increase in tensile strength compared to the Ctrl specimen, respectively. The increase is due to the pozzolanic reaction of SF and WGP with $Ca(OH)_2$, which leads to the formation of C-S-H [88]. Also, at the ages of 28, 56, and 90 days, the ternary specimen of SF5 + GGBFS10 obtained 2.1%, 14.9%, and 3.7% increase in tensile strength compared to the Ctrl specimen, respectively. The increase in tensile strength in the ternary specimen of SF5 + GGBFS10 is due to the presence of SF, which leads to a significant reduction of $Ca(OH)_2$ and improvement of the ITZ of concrete. In addition, GGBFS particles are attached to the surrounding $Ca(OH)_2$ crystals due to the pozzolanic reaction of SF [87].

In the binary specimens of WGP15 and GGBFS15, a slight decrease in tensile strength was observed at the final ages compared to the Ctrl specimen. This issue can be attributed to the decrease in the amount of cement in these specimens and the low reactivity rate of these two materials at these ages [38, 87, 88].

3.1.3. Flexural Strength. According to Figure 7, the flexural strength of the binary specimen of SF5 at the ages of 7, 28, 56, and 90 days increased by 12.3%, 11.7%, 10.3%, and 10.2%, compared to the Ctrl specimen, respectively. An increase in flexural strength was observed for ternary specimens of all ages. The increase in strength at the ages of 7, 28, 56, and 90 days in the SF5 + WGP10 specimen was 1.2%, 11.7%, 18.3%, and 19.3%, respectively, and in the SF5+GGBFS10 specimen, it was 1.2%, 9.4%, 9.1%, and 9%, compared to the Ctrl specimen, respectively.

The reaction of SiO_2 in SF with $Ca(OH)_2$ causes the formation of C-S-H gel. Increasing C-S-H gel and reducing capillary pores in cement paste is one of the main factors in increasing the strength and reducing the porosity of concrete [78, 85, 87, 88]. Similar to compressive strength and tensile strength results, for binary specimens of WGP15 and GGBFS15, a slight decrease in flexural strength was observed at the final ages.

3.2. Durability Tests

3.2.1. Magnesium Sulfate Attack. Magnesium sulfate is often found in groundwater, seawater, and some industrial effluents. Magnesium solutions easily react with $Ca(OH)_2$ in Portland cement paste to form soluble salts of calcium. Magnesium sulfate solution is the most aggressive because the sulfate ions can damage the alumina-bearing hydrates in the Portland cement paste. The characteristic feature of magnesium ion attack on cement paste is that the attack is extended to calcium silicate hydrate, which is the main component of cement. In prolonged contact with magnesium solutions, the C-S-H in Portland cement paste gradually loses its calcium ions, which are replaced by magnesium ions. The ultimate product of this substitution reaction is a magnesium silicate hydrate, the formation of which is associated with the loss of the cementitious characteristic. Due to the

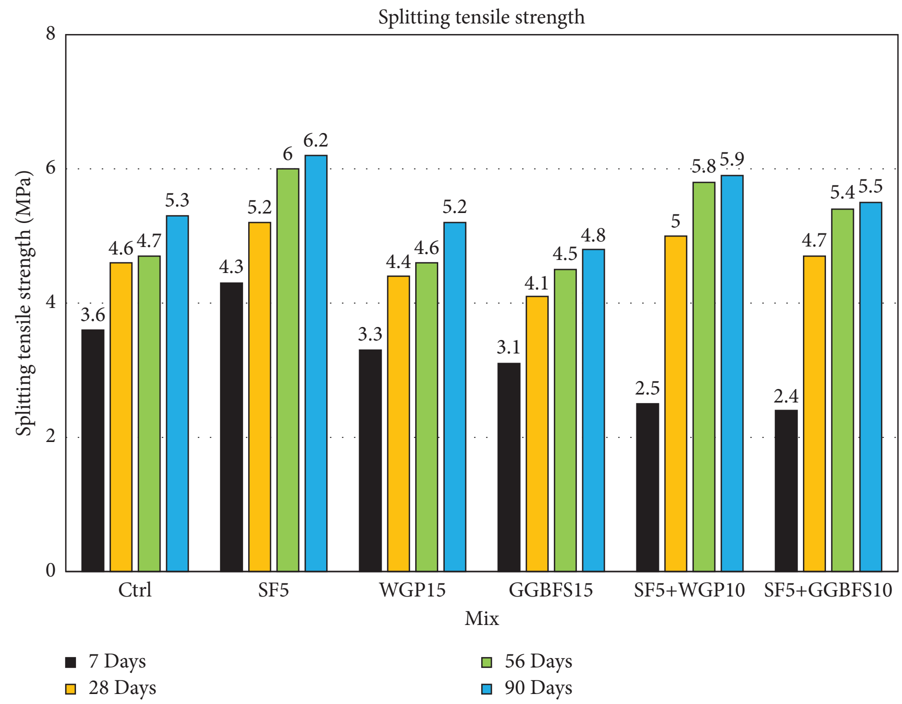

Figure 6: Tensile strength results of concrete mixtures.

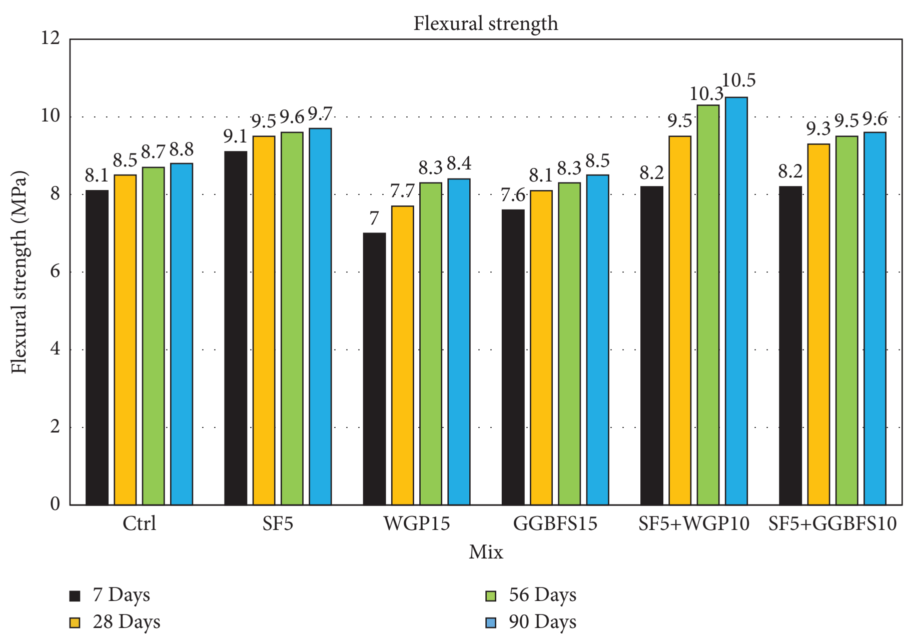

Figure 7: Flexural strength results of concrete mixtures.

presence of $Ca(OH)_2$ in the hydrated Portland cement paste, when the cement paste comes into contact with sulfate ions, alumina-containing hydrates are converted to the high-sulfate form (i.e., ettringite), which are shown in the following equations [19]:

$$C_3A \cdot CH \cdot H_{18} + 2CH + 3\overline{S} + 11H \longrightarrow C_3A \cdot 3C\overline{S} \cdot H_{32}, \quad (1)$$

$$C_3A \cdot C\overline{S} \cdot H_{18} + 2CH + 2\overline{S} + 12H \longrightarrow C_3A \cdot 3C\overline{S} \cdot H_{32}. \quad (2)$$

Gypsum formation as a result of cation-exchange reactions is also capable of causing expansion. However, it has been observed that deterioration of hardened Portland cement paste by gypsum formation goes through a process that first leads to a reduction of pH of the system and loss in stiffness and strength, followed by expansion and cracking, and finally, the transformation of the concrete into a mushy or noncohesive mass, which are shown in the following equations:

$$MgSO_4 + Ca(OH)_2 + 2H_2O \longrightarrow CaSO_4 \cdot 2H_2O + Mg(OH)_2, \quad (3)$$

$$3MgSO_4 + 3CaO\,.\,2SiO_2\,.\,3H_2O + 8H_2O \longrightarrow 3(CaSO_4\,.\,2H_2O) + 3Mg(OH)_2 + 2SiO_2\,.\,H_2O. \quad (4)$$

In the attack of magnesium sulfate and the conversion of $Ca(OH)_2$ to gypsum, it is accompanied by the simultaneous formation of $Mg(OH)_2$ (brucite), which is insoluble and reduces the alkalinity of the system. In the absence of hydroxyl ions in the pore solution, the stability of C-S-H in the system is reduced and attacked by the sulfate solution (4).

(1) Changes in Compressive Strength. In Figure 8(a), the changes in the compressive strength of the specimens exposed to magnesium sulfate are observed. Up to the age of 90 days, the compressive strength of all specimens exposed to magnesium sulfate increased compared to the initial compressive strength (i.e., 28 days cured in water).

Binary specimens of WGP15 and GGBFS15 show the highest compressive strength increase at 90 days compared to other specimens. The improvement of magnesium sulfate resistance in the binary specimen of WGP15 may be due to the sacrificial behavior of WGP. WGP produces compounds that are not as harmful as those formed by the decomposition of cement hydration products exposed to the magnesium sulfate environment [62, 98]. WGP leaches alkali ions of Na^+ and Si^+ into the solution, which leads to the neutralization of magnesium sulfate. In addition, the pozzolanic reaction of WGP increases the alkaline concentration of the pore solution [89, 99], which prevents the decomposition of hydration products by magnesium sulfate. Mostofinejad et al. [63] reported that the incorporation of recycled concrete aggregates with WGP leads to significant improvements in the development of concrete compressive strength in the magnesium sulfate environment with saturated concentration (i.e., 14.7%) [63]. Liu et al. [100] also reported that replacing fine aggregate with a liquid crystal display (LCD) improves the performance of concrete against sulfate attacks. They pointed out that glass powder has low water absorption, which leads to an increase in the effective water-cement ratio of the concrete mixture, which causes increased porosity and provides sufficient space for salt to crystallize before damaging the cement matrix [100].

In the binary specimen of GGBFS15, the resistance to magnesium sulfate was increased due to the decrease in the content of C_3A, $Ca(OH)_2$, and the penetrability of concrete. GGBFS consumes less $Ca(OH)_2$ than other SCMs and usually reduces the penetrability of concrete due to improved pore structure [101, 102]. In addition, the behavior of GGBFS depends on the replacement level and its chemical composition; in concrete mixtures, good behavior is usually observed when the replacement level of GGBFS is high (i.e., 70%). This behavior is amplified when the GGBFS has a lower content of (Al_2O_3). Hooton and Emery [103], Gollop and Taylor [104, 105], Locher [106], Higgins [107], Ogawa et al. [108], Whittaker and Black [109], and Mostofinejad et al. [67] reported that GGBFS could contribute to the resistance of concrete against sulfate attack [67, 103–109].

According to the changes in compressive strength at the age of 90 days, it was observed that SF5, SF5+WGP10, and SF5+GGBFS10 specimens have less resistance to magnesium sulfate attack than the Ctrl specimen. Partial replacement of cement by SF reduces the availability of $Ca(OH)_2$ due to the pozzolanic reaction and allows magnesium sulfate to more easily attack C-S-H, leading to decalcification, formation of M-S-H, and destruction of the cement bond [110–113]. Similar studies by Baghabra Al-Amoudi [111], Ganjian and Pouya [112], Lee et al. [113], Mostofinejad et al. [67], and Ortega et al. [114] confirm the significant decrease in compressive strength of concretes containing SF against magnesium sulfate attack [67, 111–114].

(2) Changes in Weight. The results of weight changes of concrete specimens exposed to magnesium sulfate solution are presented in Figure 8(b). The presented results show that all the specimens gained weight for up to 90 days. The increase in weight in concrete specimens is due to the formation of gypsum and ettringite, which is the result of the reaction of magnesium sulfate with $Ca(OH)_2$, C_3A, and C_4AF [77, 114].

In general, the specimens containing SF had the lowest weight gain. As we know, SF pozzolanic reactions lead to a decrease in $Ca(OH)_2$ content, and this issue decreases the potential of gypsum and ettringite formation. Based on the results of other mechanical and durability tests in this study, the positive effect of particle packing or space-filling of SF was observed [79, 80, 82]. Therefore, the ternary specimens of SF5 + WGP10 and SF5 + GGBFS10 containing SF have lower penetrability than the binary specimens of WGP15 and GGBFS15 without SF. By reducing the penetrability, the diffusion of sulfate ions in concrete is decreased [77, 111, 114]. However, reducing the pore volume does not always guarantee acceptable performance against magnesium sulfate attacks because the arrangement of these pores is also important [64]. The destructive effect of magnesium sulfate in concrete containing SF is related to the difference in the reaction mechanisms and the attack of magnesium sulfate, which causes a further reduction of alkalinity by the

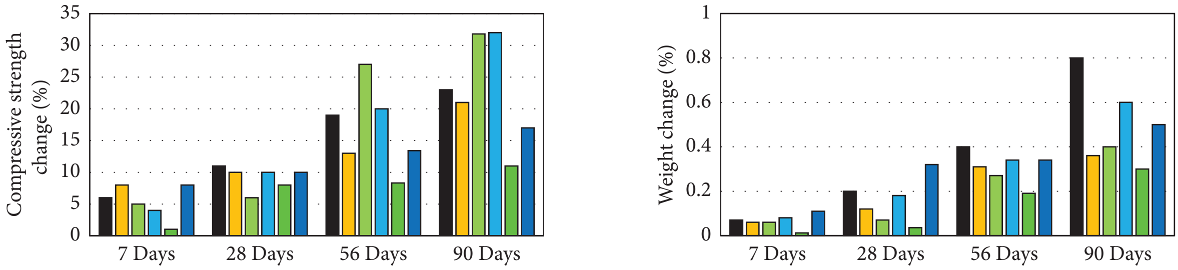

	7 Days	28 Days	56 Days	90 Days
Ctrl	6	11	19	23
SF5	8	10	13	21
WGP15	5	6	27	31.8
GGBFS15	4	10	20	32
SF5+WGP10	1	8	8.3	11
SF5+GGBFS10	8	10	13.4	17

(a)

	7 Days	28 Days	56 Days	90 Days
Ctrl	0.07	0.2	0.4	0.8
SF5	0.06	0.12	0.31	0.36
WGP15	0.06	0.07	0.27	0.4
GGBFS15	0.08	0.18	0.34	0.6
SF5+WGP10	0.012	0.036	0.19	0.3
SF5+GGBFS10	0.11	0.32	0.34	0.5

(b)

Figure 8: (a) Compressive strength changes of concrete after exposure to magnesium sulfate. (b) Weight changes of concrete after exposure to magnesium sulfate.

pozzolanic reactions of SF, which eventually leads to the decomposition of C-S-H and excessive reduction of strength [77]. Banar et al. [77], Hendi et al. [64], Hekal et al. [115], Baghabra Al-Amoudi [111], and Torii and Kawamura [116] observed a similar effect of SF on pore refinement, but they believed that there is no clear justification for the positive effect of SF on resistance to magnesium sulfate, and using the weight change factor to predict resistance to magnesium sulfate attack is not an accurate method [64, 77, 111, 115, 116].

The lower weight gain of the binary specimen of WGP15 compared to the Ctrl specimen is related to the reduction of C_3A due to the decrease in the extent of cement and the consumption of $Ca(OH)_2$ due to the pozzolanic reaction, which ultimately reduces the formation of gypsum and ettringite. In addition, the reaction of magnesium sulfate with WGP produces compounds with a lower density than the reactants, which might be why the binary specimen of WGP15 does not show the same weight gain shown by the other specimens [62]. Mostofinejad et al. [63] evaluated the durability of concrete containing recycled concrete aggregates with WGP in the magnesium sulfate environment. They reported that adding 30% WGP to concrete containing recycled concrete aggregates improved the performance of concrete in the magnesium sulfate environment [63]. Hendi et al. [64], in another study, investigated the performance of concrete containing 6%, 13%, and 20% WGP in the magnesium sulfate environment with a fully saturated concentration. They reported that after 150 days of exposure to magnesium sulfate, all specimens containing WGP showed less weight gain than the Ctrl specimen [64].

The binary specimen of GGBFS15 showed a lower weight gain than the Ctrl specimen after 90 days of exposure to magnesium sulfate. Nevertheless, compared to other specimens, it showed more weight gain. SCMs are usually deficient in calcium compared to cement [102]. Hydrated SCMs further decrease the $Ca(OH)_2$ content. GGBFS may also consume $Ca(OH)_2$ but to a lesser value [109]. Due to the lower consumption of $Ca(OH)_2$ by GGBFS, the potential of gypsum and ettringite formation in concrete containing GGBFS is higher than that of concrete containing WGP and SF. Therefore, the higher weight gain of the binary specimen of GGBFS15 than other specimens containing WGP and SF can be predicted. In an investigation, Durgun and Sevinç [117] determined the effectiveness of pumice, waste glass powder, GGBFS, and colemanite waste against sodium and magnesium sulfate attacks; they reported that the most effective mineral additive to reduce the weight loss of concrete specimens is GGBFS, which has an optimal usage rate of 10%, and the worst case is when GGBFS is not used in the mix design. Finally, the results showed that the ideal mixing ratio to minimize weight loss due to sulfate attack is 5% pumice, 5% waste glass powder, 10% GGBFS, and 1% colemanite waste [117].

3.2.2. Sulfuric Acid Attack. Effluents from furnaces that use high-sulfur fuels and effluents from chemical industries may contain sulfuric acid. The loss of organic matter in marshes, shallow lakes, mining pits, and sewage pipes often results in the formation of H_2S, which can be converted to sulfuric acid by bacterial action. Therefore, it is necessary to investigate the performance of concrete in acidic environments.

In a well-hydrated concrete, the cement paste phase, comprised of moderately insoluble hydrates of calcium (C-S-H, $Ca(OH)_2$, and the AFt and AFm phases), exists in a state of stable balance with a high-pH pore solution. Depending on the Na^+, K^+, and OH^- ions concentration, the *pH* value ranges from 12.5 to 13.5. Less than 12.5 *pH* theoretically leads to instability of the cementitious products of hydration; this means that most natural waters and urban wastewater are damaging to concrete. The rate of chemical attack depends on the *pH* and penetrability of concrete, so in concrete with low penetrability and *pH* above 6, the rate of chemical attack is too slow [19, 118].

On the other hand, by reducing the concentration of Ca^{2+} ions in the pore solution, the chemical balance of the cement paste is disturbed, which first damages the $Ca(OH)_2$ and then the C-S-H gel [119]. The reaction of sulfuric acid with components of hydrated cement paste is shown in (5) and (6). In the next step, ettringite could be formed through the chemical reaction between gypsum and some hydration products such as monosulfate, calcium aluminate hydrate, and unhydrated tricalcium aluminate (C_3A). These reactions are sulfate attacks (equations (7)–(9)). It should be noted that the reactions of ettringite production increase the volume, which creates cracks in concrete, and the damage caused by the sulfuric acid attack is intensified [19, 119].

$$H_2SO_4 + Ca(OH)_2 \longrightarrow CaSO_4 + 2H_2O, \tag{5}$$

$$H_2SO_4 + CaO.SiO_2 . 2H_2O \longrightarrow CaSO_4 + Si(OH)_4 + H_2O, \tag{6}$$

$$3CaO . Al_2O_3 . CaSO_4 . 12H_2O + 2CaSO_4 . 2H_2O + 16H_2O \longrightarrow 3CaO . Al_2O_3 . 3CaSO_4 . 32H_2O, \tag{7}$$

$$3CaO . Al_2O_3 . Ca(OH)_2 . 12H_2O + 3CaSO_4 . 2H_2O + 13H_2O \longrightarrow 3CaO . Al_2O_3 . 3CaSO_4 . 32H_2O + Ca(OH)_2, \tag{8}$$

$$3CaO . Al_2O_3 + 3CaSO_4 + 32H_2O \longrightarrow 3CaO . Al_2O_3 . 3CaSO_4 . 32H_2O. \tag{9}$$

(1) Changes in Compressive Strength. Figure 9(a) shows the changes in the compressive strength of the specimens after exposure to sulfuric acid. The results show that all specimens decreased compressive strength up to 90 days. Changes in compressive strength depend on the formation of chemical products in exposure to the sulfuric acid solution. The decrease in compressive strength in all specimens containing SF, WGP, and GGBFS was higher than in the Ctrl specimen. The Ctrl specimen has more potential in gypsum and ettringite formation than other specimens due to the higher content of $Ca(OH)_2$ and C_3A. Filling concrete pores with gypsum and ettringite improves compressive strength in the short term [98].

The binary specimen of WGP15, after 90 days of exposure to the sulfuric acid solution, showed the best performance compared to other binary and ternary specimens. The lower reduction of the compressive strength of the binary specimen of WGP15 can be related to the high porosity of the cement paste, which has more pores for the formation of gypsum and ettringite because these products act as fillers at early ages and improve the compressive strength of the concrete specimens.

In addition, the lower reduction of the compressive strength of the binary specimen of WGP15 can be due to the sacrificial nature of the WGP, which produces chemical compounds that are nonexpandable in nature and have less damage than ettringite. Due to the sacrificial nature of WGP, the rate of ettringite formation is reduced. By acting as a sacrificial material, WGP prevented the disintegration of C-S-H and C-A-S-H compounds, thus reducing the intensity of loss in compressive strength [62, 98]. Bisht et al. [98] also reported that when 24% of waste glass (150–600 μm) was replaced by river sand, the resistance of concrete against sulfuric acid attack is improved. Even after 90 days of exposure to sulfuric acid, the compressive strength was 54% higher than plain concrete [98]. Jain et al. [120] also stated that adding glass powder up to 15% to plain concrete improved the resistance against sulfuric acid attack. Concrete containing 15% glass powder showed the best performance after 84 days of exposure to a 3% sulfuric acid solution [120].

The binary specimen of GGBFS15 showed acceptable performance at early ages. GGBFS creates the least pore ratio due to improving the pore structure of concrete [101, 102]. Therefore, any slight formation of gypsum and ettringite contributes to the easy filling of the pores, which leads to an increase in compressive strength; nevertheless, after 28 days of exposure to sulfuric acid, loss of compressive strength was observed; because the formed products need high volume, it leads to simultaneous expansion and cracking, and it facilitates the ingress of sulfuric acid; as a result, the compressive strength of concrete loses over time [62, 121]. The study of Sturm et al. [121] evaluated the resistance of one-part geopolymer mortars against sulfuric acid. They reported that adding 25 wt% of GGBFS reduced the resistance against sulfuric acid by forming expanded calcium sulfate phases [121].

As mentioned earlier, SF significantly improved the mechanical properties and reduced the porosity of concrete. However, specimens containing SF showed a weaker performance than other specimens after 90 days of exposure to the sulfuric acid solution. Thus, it can be argued that converting $Ca(OH)_2$ to C-S-H and refining the porosity of concrete are not effective in preventing the loss of compressive strength against sulfuric acid attack [122]. Due to the reduction of concrete porosity, any slight formation of gypsum and ettringite leads to internal stresses and premature cracking. In the next step, sulfuric acid attacks C-S-H easier and faster due to the reduction of the availability of $Ca(OH)_2$, which causes the instability of the cement paste and loss of strength [123].

The results of the current study showed that higher compressive strength does not necessarily guarantee the durability of concrete against the attack of magnesium sulfate and sulfuric acid. The results of this study are in

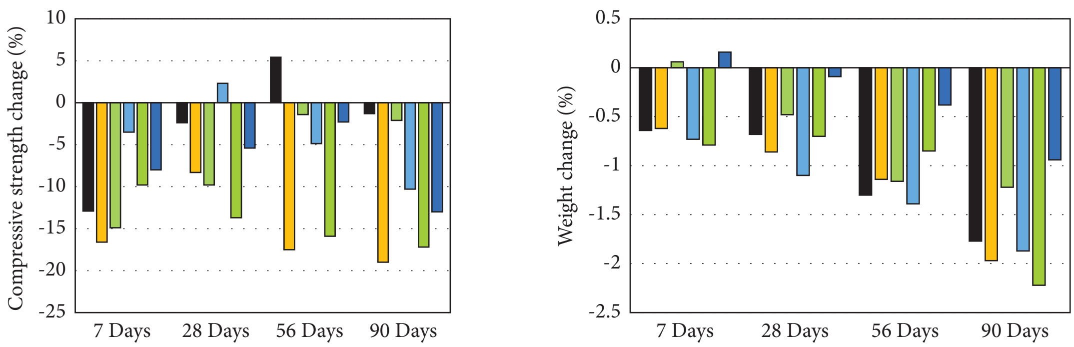

	7 Days	28 Days	56 Days	90 Days
Ctrl	-12.9	-2.38	5.41	-1.3
SF5	-16.6	-8.3	-17.5	-19
WGP15	-14.9	-9.8	-1.4	-2.1
GGBFS15	-3.5	2.3	-4.86	-10.3
SF5+WGP10	-9.8	-13.7	-15.9	-17.2
SF5+GGBFS10	-8	-5.4	-2.3	-13

(a)

	7 Days	28 Days	56 Days	90 Days
Ctrl	-0.64	-0.68	-1.3	-1.77
SF5	-0.62	-0.86	-1.14	-1.97
WGP15	0.06	-0.48	-1.16	-1.22
GGBFS15	-0.73	-1.1	-1.39	-1.87
SF5+WGP10	-0.79	-0.7	-0.85	-2.22
SF5+GGBFS10	0.16	-0.09	-0.38	-0.94

(b)

Figure 9: (a) Compressive strength changes in concrete after exposure to sulfuric acid. (b) Changes in concrete weight after exposure to sulfuric acid.

accordance with the findings of Senhadji et al. [122]. They found that cement mortar and mortars containing natural pozzolan and limestone showed better performance against sulfuric acid attack compared to mortar containing SF [122]. Torii and Kawamura [116] also reported that the partial replacement of Ordinary Portland Cement by SF and fly ash could not effectively prevent the destruction of concrete by sulfuric acid involving the scaling and softening [116].

(2) Changes in Weight. Figure 9(b) shows the changes in the weight of the specimens after exposure to sulfuric acid. Based on the results, all specimens lost weight after 90 days. The ternary specimen of SF5 + GGBFS10 showed the lowest weight loss compared to other specimens, which may be due to the pozzolanic reaction of SF, which reduced the $Ca(OH)_2$ content and formed more C-S-H. But the binary specimen of GGBFS15 has a higher potential for gypsum and ettringite formation due to the extent of consumption of less $Ca(OH)_2$, so expansion and cracking lead to rupture and weight loss.

The binary specimen of WGP15 also showed a lower weight loss than the Ctrl specimen, which may be related to the higher porosity of the cement paste and the sacrificial nature of the WGP. As mentioned earlier, WGP produces compounds that are nonexpansive in nature and are not as damaging as ettringite, consequently reducing internal stresses that lead to cracking and preventing rupture and weight loss [62, 98].

The negative effect of using SF on the weight changes of SF5 + WGP10 and SF5 specimens was observed. This behavior may be attributed to the lower porosity of the cement paste because the pore refinement by SF reduces the concrete pore volume. Undoubtedly, the pore volume is one of the most effective parameters in improving the resistance of concrete against sulfuric acid attacks. Because the higher pore volume provides more accessible spaces for the formation of gypsum and ettringite, and as a result, internal stresses and intense damage are prevented [123].

According to the results of the current study, the results reported by Hendi et al. [123], Bassuoni and Nehdi [124], Chang et al. [125], and De Belie et al. [126] found that there is no direct correlation between compressive strength changes and weight changes after exposure to the sulfuric acid solution [123–126].

3.2.3. Surface Resistivity. The resistivity of concrete is an essential parameter in the corrosion of reinforced concrete structures. High-resistivity concrete has little possibility of developing reinforcement corrosion. In the field, the electrical resistivity is determined by measuring the potential differences at the concrete surface caused by injecting a small current at the surface [19]. Electrical resistivity indicates the mobility of ions throughout the concrete matrix [127]. The higher the penetrability of the concrete, the easier and faster the ions penetrate into the concrete. If the concrete has higher electrical resistance and lower penetrability, it has a better resistance against destructive ions such as chloride [128, 129].

According to Figure 10, the surface resistivity for all specimens containing SF increased higher than 200% in the early ages and up to 300% in the final ages compared to the Ctrl specimen; the positive effect of using SF in increasing the surface resistivity was confirmed by the authors of [82, 83, 127–130]. According to Table 3, presented by AASHTO-T 358, the chloride ion penetration for specimens of SF5, SF5 + WGP10, and SF5 + GGBFS10 was in the very low range.

At the age of 120 days, the surface resistivity of the binary specimens of WGP15 and GGBFS15 was increased by 94.7% and 73.6% compared to the Ctrl specimen, respectively. The chloride ion penetration was in the low range, while in the Ctrl specimen, the chloride ion penetration remained in the moderate range for 120 days. This matter shows the positive effect of SCMs in improving the density of cement paste

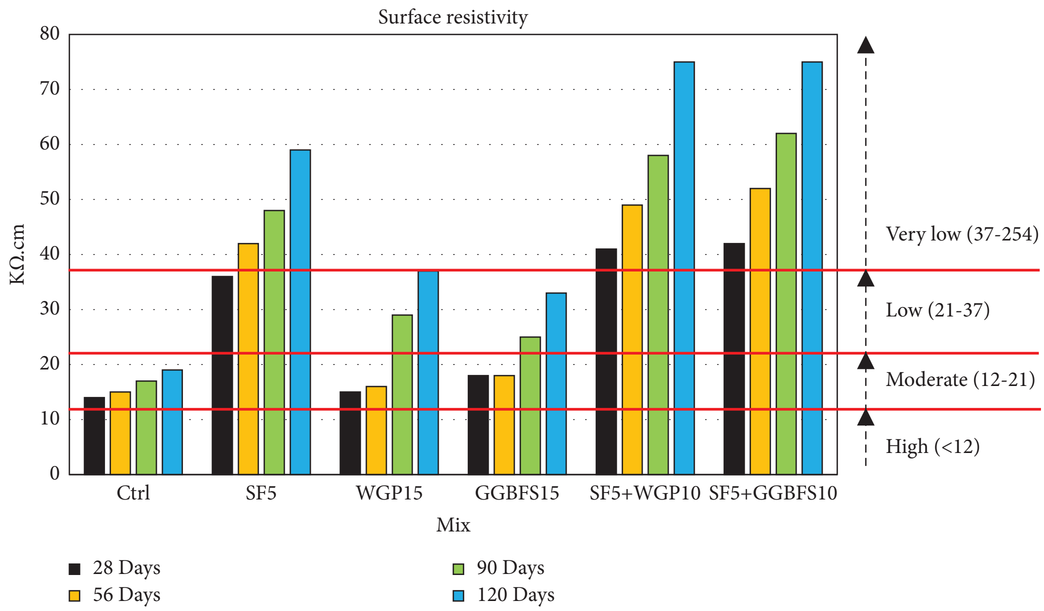

FIGURE 10: Surface resistivity results of concrete mixtures.

TABLE 3: Chloride ion penetration based on AASHTO-T 358.

Chloride ion penetration	Surface resistivity (KΩ·cm)
High	<12
Moderate	12–21
Low	21–37
Very low	37–254
Negligible	>254

structure and reducing the volume of capillary pores due to the pozzolanic reaction.

Mehta and Monteiro [19] stated that the risk of reinforcement corrosion increases with the reduction of the electrical resistance of concrete. Nevertheless, as long as the electrical resistance of concrete is above 50 to 70 KΩ·cm, significant corrosion is not observed [19].

The risk of reinforcement corrosion was significantly reduced in the ternary specimens of SF5 + WGP10 and SF5 + GGBFS10 due to the electrical resistance above 70 KΩ·cm.

3.2.4. Rapid Chloride Penetrability Test (RCPT). Fluctuations in temperature and humidity, short-term and long-term internal chemical reactions, and pores geometry in concrete all contribute to chloride ion penetration rates [131]. The RCPT result is interpreted as an indicator of electrical conductivity [86]. In this test, the accumulated charges passing through the specimens are measured, which determines the chloride ion penetrability of concrete. Electrical conductivity is sensitive to the flow of ions released in the cementitious products of hydration through the water in the pores. The lower the electrical conductivity of the concrete, the lower the current flowing between the anodic and the cathodic areas, and thus, the lower rate of corrosion. Hence, the risk of reinforcement corrosion can be evaluated by measuring the electrical conductivity of concrete [132, 133].

RCPT results are shown in Figure 11. The overall results are similar to surface resistivity. As can be seen, due to the completion of hydration, the amount of charges passing decreases at the final age. According to the classification presented in the ASTM C1202 standard (Table 4), it can be stated that the chloride ion penetrability in the specimens of SF5, SF5+WGP10, and SF5+GGBFS10 after 56 days is very low. The very fine particles of SF, the high rate of pozzolanic reaction, and the filling effect can reduce the pore volume and increase the homogeneity of concrete, thus hindering the mobility and interaction of ions [127, 128, 134].

The high amount of charges passing at the age of 28 days in the binary specimen of GGBFS15 is probably due to the low rate of pozzolanic reaction. Because after the age of 56 days, due to the progress of the pozzolanic reaction that leads to the densification of the pore structure, the amount of charges passing shows a significant decrease [135]. Finally, at the age of 120 days, the chloride ion penetrability was in the low range.

The highest amount of charges passing is at the age of 28 days in the binary specimen of WGP15. It is well known that RCPT is basically an electrical conductivity or resistivity test, and the conductivity of the pore solution also affects the results of this test. The presence of a pore solution with higher conductivity leads to a higher apparent amount of charges passing even if the microstructure is the same. Based on the studies of Du and Tan [86], Zheng [89], Jain and Neithalath [136], it was observed that due to its high Na_2O and SiO_2, glass powder releases a large amount of alkaline content in the pore solution and thus increases the conductivity of the pore solution [86, 89, 136]. But at the ages of 56, 90, and 120 days, a significant decrease in charges passing was observed; because of the cement hydration reaction, a pore solution rich in Ca^{2+}, SiO_4^{2-},

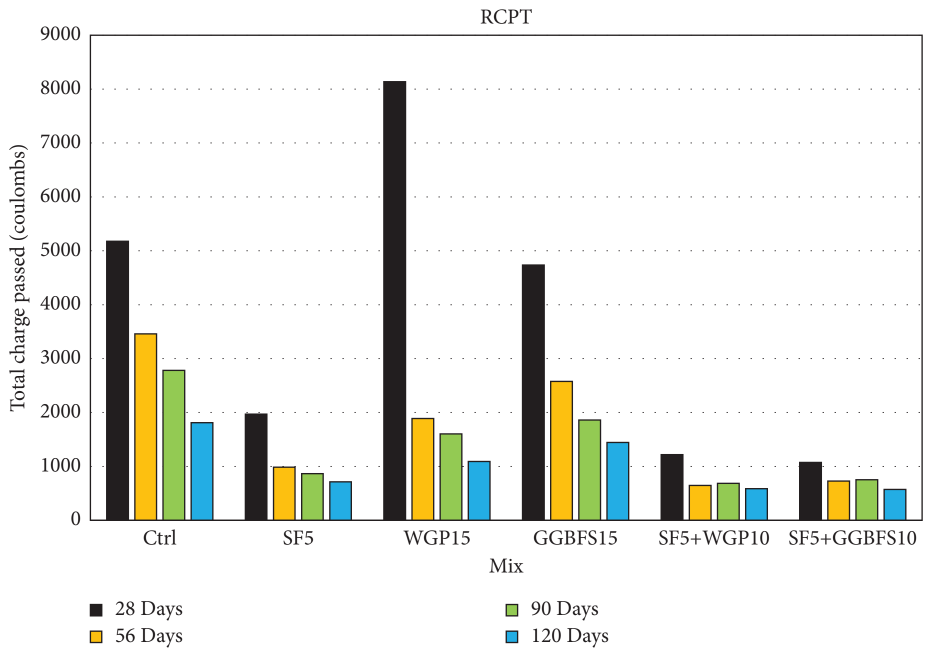

Figure 11: Rapid chloride penetrability test (RCPT) results of concrete mixtures.

Table 4: Chloride ion penetrability based on ASTM C1202.

Chloride ion penetrability	Charge passed (coulombs)
High	>4000
Moderate	2000–4000
Low	1000–2000
Very low	100–1000
Negligible	<100

and OH^- ions is produced, and the amorphous silica present in (Si-O-Si bond) glass powder can dissolve under this high *pH* solution and form a layer rich in Si^+ on the surface of the glass powder. This layer reacts with Ca^{2+} ions in the solution and turns into C-S-H; this formed C-S-H has a lower Ca/Si ratio and thus absorbs more Na^+ released from the glass powder [86, 137]. Consequently, the improved microstructure and the decrease in the concentration of ions in the pore solution lead to a decrease in electrical conductivity [86]. Eventually, at the age of 120 days, the chloride ion penetrability in the binary specimen of WGP15 was in the low range.

The investigation of Yeau and Kim [135], Kayali et al. [134], Pilvar et al. [127], Du and Tan [86], and Delnavaz et al. [128] confirmed that the addition of FS, WGP, and GGBFS to concrete is effective in reducing chloride ion penetrability and increases the durability of concrete in chloride corrosive environments [86, 127, 128, 134, 135].

3.2.5. Water Absorption. The water absorption test provides information on capillarity suction and is a standard indicator for measuring the resistance of concrete when exposed to aggressive environments. The durability of concrete is significantly affected by water movement in concrete [138]. Water absorption is generally affected by pore structure, porous paste, and ITZ, and these factors are essential at early ages [19].

Figure 12 shows the results of water absorption after 30 minutes (initial absorption) and 24 hours (final absorption) at the ages of 28, 56, 90, and 120 days. According to the results, it can be seen that the initial and final water absorption at the age of 120 days is lower for SF5, SF5 + WGP10, and SF5 + GGBFS10 specimens than other specimens. The decrease in water absorption can be attributed to the pozzolanic reaction of SF and converted interconnected pores to unconnected pores. As a result, the porosity of cement paste decreases. The results obtained by Yusuf et al. [10], Gupta et al. [139], Khaloo et al. [140], Madani et al. [41], and Sabet et al. [141] confirmed that the use of SF in concrete reduces water absorption [10, 41, 139–141].

At the ages of 56, 90, and 120 days, the binary specimens of WGP15 and GGBFS15 showed good performance compared to the Ctrl specimen; due to the pozzolanic reaction and particle packing, the porosity decreased and led to low water absorption.

CEB [142] recommends water absorption after 30 minutes (initial absorption). According to CEB recommended limits, water absorption of all concrete specimens was less than 3%, indicating good concrete durability [142]. Shetty and Jain [143] believe that high-quality concrete has a final absorption of less than 5% [143]. Based on the results, all mixtures can be considered high-quality concrete in water absorption.

3.2.6. Depth of Penetration of Water under Pressure. Another method of measuring concrete penetrability is the depth of penetration of water. Water penetration into concrete can cause physical and chemical damages. Water as a solvent can dissolve many cement components [144]. Many ions cause damage to concrete by water penetration. Therefore, water penetration in concrete can be used as an indicator of concrete

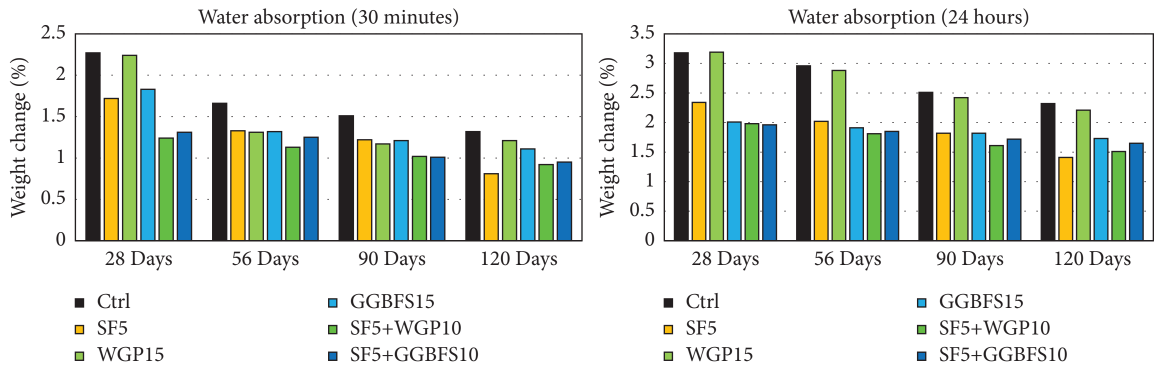

Figure 12: Water absorption test results of concrete mixtures.

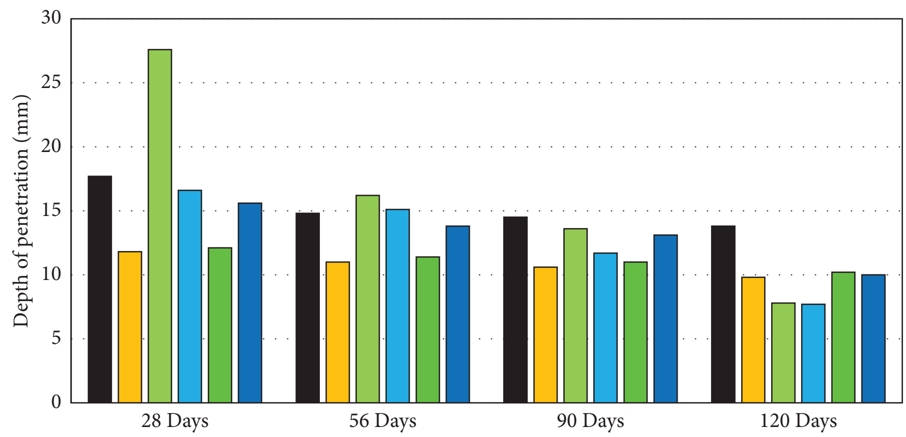

	28 Days	56 Days	90 Days	120 Days
Ctrl	17.7	14.8	14.5	13.8
SF5	11.8	11	10.6	9.8
WGP15	27.6	16.2	13.6	7.8
GGBFS15	16.6	15.1	11.7	7.7
SF5+WGP10	12.1	11.4	11	10.2
SF5+GGBFS10	15.6	13.8	13.1	10

Figure 13: Depth of penetration of water under pressure results of concrete mixtures.

durability [82, 145]. The penetrability of concrete is influenced by the total volume, shape, and connectivity of the pores [146].

In this study, the average depth of penetration measure was reported. Motahari Karein et al. [129] and Banar et al. [77] reported that using the average depth of penetration of water is an acceptable measurement and illustrates more accurate results. During the test, it was observed that the depth of penetration of water could be artificially increased locally due to the presence of aggregates near the surface of the specimen under water pressure [77, 129]. According to Mindess et al. [147], the depth of penetration of water indicates the total volume of open pores larger than 100 nm. Open pores are pathways for water penetration and ions in the concrete system [147].

The results of the depth of penetration of water test at the ages of 28, 56, 90, and 120 days are shown in Figure 13. The depth of penetration of water for all specimens containing SF decreased compared to the Ctrl specimen. This decrease in penetration depth at the age of 120 days in the SF5, SF5 + WGP10, and SF5 + GGBFS10 specimens is 29%, 26%, and 27.5%, respectively. The reduction of depth of penetration of water at early ages in ternary specimens of SF5 + WGP10 and SF5 + GGBFS10 is due to the presence of SF. Due to its very fine particles and the high rate of pozzolanic reaction at early ages, SF improves the microstructure and densification of the ITZ, which partially blocks the paths of water penetration [139]. Based on the results obtained from Ahmad et al. [148], Ince et al. [149], and Gupta et al. [139] researches, the positive effect of using SF in reducing the depth of penetration of water was confirmed [139, 148, 149].

The binary specimens of WGP15 and GGBFS15 exhibited weak performance at early ages, but at the age of 120 days, 43% and 44.2% reduction in the depth of penetration of water was observed compared to the Ctrl specimen, respectively, which shows the best performance among all specimens. According to the results of other researchers, the use of WGP and GGBFS has positive effects on the mechanical properties and durability of concrete. Because of the pozzolanic reaction, the porosity decreases, and a smaller pore structure is created

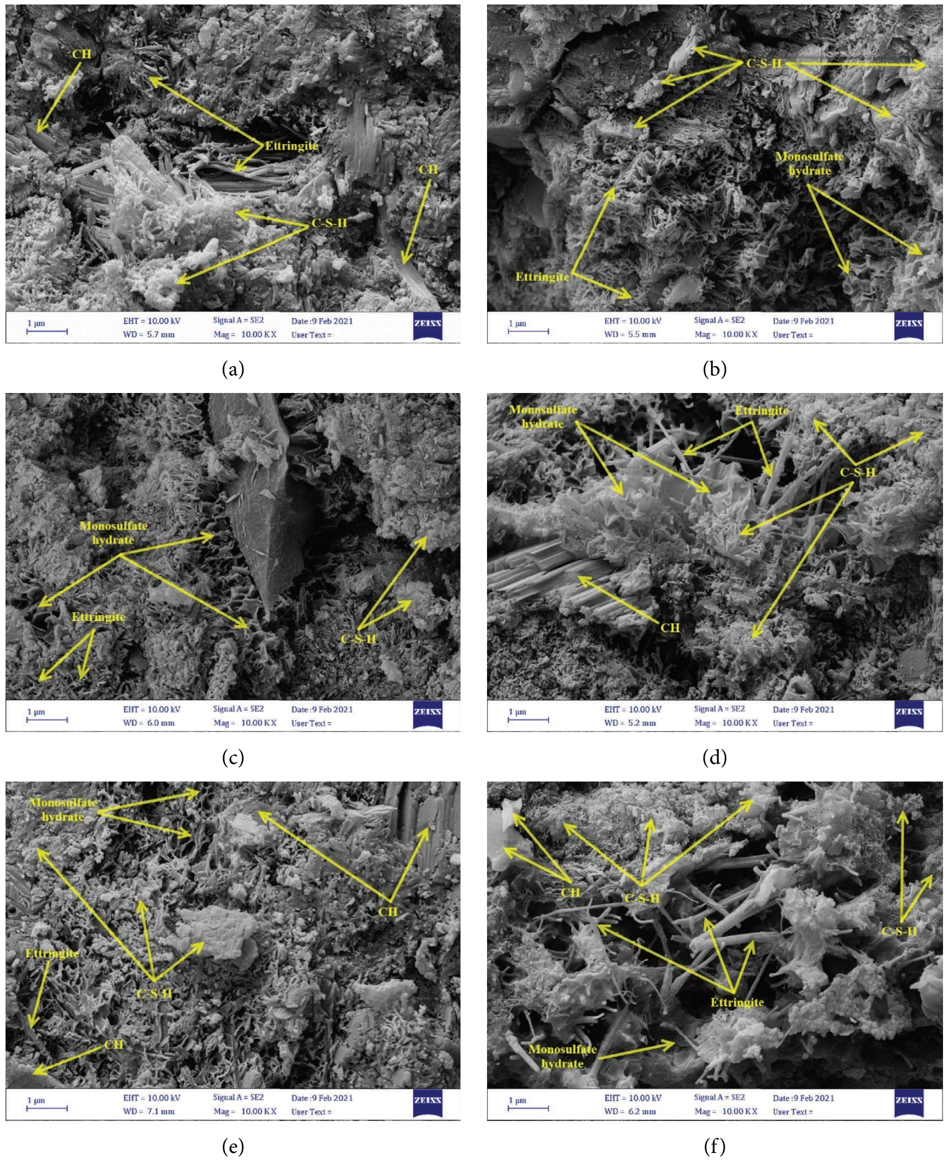

Figure 14: SEM images of the concrete specimens after 90 days of curing. (a) Ctrl. (b) SF5. (c) WGP15. (d) GGBFS15. (e) SF5 + WGP10. (f) SF5 + GGBFS10.

in the concrete nucleus, which leads to a decrease in the depth of penetration of water [86, 150, 151].

3.2.7. SEM Analysis. Figure 14 shows the images of SEM. To understand the cause, rate, and mechanism of destruction, or how to improve some properties of concrete, complete knowledge of the microstructure of hardened concrete is necessary. The mechanical properties of concrete often depend on its microstructure. Cement paste contains products of cement hydration, which is 50–60% of the solid volume of cement paste containing C-S-H, 20–25% including $Ca(OH)_2$ crystals, and the rest including AFt (i.e., ettringite), AFm (i.e., monosulfate), unhydrated cement, and the porosity of cement paste [152]. As shown in Figure 14, the presence of SF has a positive effect on the microstructure of concrete and has helped to improve the packing density and structure of the cement paste [82].

4. Conclusions

The current study evaluated the mechanical and durability properties of concrete containing SF, WGP, and GGBFS. The main concluded remarks are as follows:

(1) Adding 5% SF to concrete mixtures containing 10% GGBFS or 10% WGP increased the compressive, tensile, and flexural strength compared to

plain concrete. Due to particle packing or space-filling, SF can fill the voids and improve the characteristics of the ternary concrete mixtures; hence, an increase in strength in the ternary concrete mixtures indicates the synergistic effect of these materials.

(2) The binary concrete mixtures containing 15% WGP or 15% GGBFS showed the best performance against the magnesium sulfate attack. Although the positive effect of adding 5% SF to concrete mixtures was observed in other mechanical and durability tests, adding SF decreased the performance of concrete against the magnesium sulfate attack.

(3) The binary concrete mixture containing 15% WGP showed good performance against the sulfuric acid attack. By acting as a sacrificial material, WGP prevented the disintegration of C-S-H and C-A-S-H compounds. All concrete mixtures containing SF showed a decrease in performance similar to the magnesium sulfate attack.

(4) Based on the surface resistivity and the RCPT results, all the binary and ternary concrete mixtures showed an increase in electrical resistivity and a decrease in electrical conductivity compared to plain concrete at the age of 120 days. Chloride ion penetrability of the ternary concrete mixtures was in the very low range, which showed the best performance. In addition, the ternary concrete mixtures are high-resistivity concrete, and there is no risk of reinforcement corrosion.

(5) The water absorption of all the binary and ternary concrete mixtures decreased compared to plain concrete because the porosity of concrete decreased due to the pozzolanic reaction and particle packing. It should be noted that the 24-hour water absorption of all concrete mixtures was less than 5%, which can be considered high-quality concrete. The depth of penetration of water under pressure has the same results. The lowest depth of penetration at the age of 120 days was related to the binary concrete mixtures of 15% WGP and 15% GGBFS, which showed a decrease of about 45% compared to plain concrete.

Data Availability

Data are available upon request of the author.

Conflicts of Interest

All authors declare that there are no conflicts of interest.

References

[1] Z. Kalakada, J. H. Doh, and S. Chowdhury, "Glass powder as replacement of cement for concrete – an investigative study," *European Journal of Environmental and Civil Engineering*, vol. 26, no. 3, pp. 1046–1063, 2022.

[2] S. Alla, M. Jayaram, and S. S. Asadi, "An experimental investigation for replacements of river sand and cement with Robosand, fly-ash and silica fume in concrete to evaluate the influence in durability properties," *Materials Today Proceedings*, vol. 43, pp. 954–961, 2021.

[3] A. M. Matos and J. Sousa-Coutinho, "Durability of mortar using waste glass powder as cement replacement," *Construction and Building Materials*, vol. 36, pp. 205–215, 2012.

[4] M. Limbachiya, M. S. Meddah, and Y. Ouchagour, "Use of recycled concrete aggregate in fly-ash concrete," *Construction and Building Materials*, vol. 27, no. 1, pp. 439–449, 2011.

[5] M. F. Alnahhal, U. J. Alengaram, M. Z. Jumaat, M. A. Alqedra, K. H. Mo, and M. Sumesh, "Evaluation of industrial by-products as sustainable pozzolanic materials in recycled aggregate concrete," *Sustainability*, vol. 9, no. 5, p. 767, 2017.

[6] L. M Federico and S. E. Chidiac, "Waste Glass-A Supplementary Cementitious Material (Doctoral Dissertation)," *Cement and Concrete*, vol. 31, no. 8, pp. 606–610, 2013.

[7] B. Pekmezci and S. Akyüz, "Optimum usage of a natural pozzolan for the maximum compressive strength of concrete," *Cement and Concrete Research*, vol. 34, no. 12, pp. 2175–2179, 2004.

[8] E. M. Golafshani and A. Behnood, "Estimating the optimal mix design of silica fume concrete using biogeography-based programming," *Cement and Concrete Composites*, vol. 96, pp. 95–105, 2019.

[9] C. S. Poon, S. C. Kou, and L. Lam, "Compressive strength, chloride diffusivity and pore structure of high performance metakaolin and silica fume concrete," *Construction and Building Materials*, vol. 20, no. 10, pp. 858–865, 2006.

[10] M. O. Yusuf, K. A. A. Al-Sodani, A. H. AlAteah et al., "Performances of the synergy of silica fume and waste glass powder in ternary blended concrete," *Applied Sciences*, vol. 12, no. 13, Article ID 6637, 2022.

[11] M. N. N. Khan, J. C. Kuri, and P. K. Sarker, "Effect of waste glass powder as a partial precursor in ambient cured alkali activated fly ash and fly ash-GGBFS mortars," *Journal of Building Engineering*, vol. 34, Article ID 101934, 2021.

[12] M. Y. Durgun and A. H. Sevinç, "High temperature resistance of concretes with GGBFS, waste glass powder, and colemanite ore wastes after different cooling conditions," *Construction and Building Materials*, vol. 196, pp. 66–81, 2019.

[13] V. M. Malhotra and P. K. Mehta, *Pozzolanic and Cementitious Materials*, CRC Press, Boca Raton, Florida, US, 2014.

[14] S. Chandra Paul, B. Šavija, and A. J. Babafemi, "A comprehensive review on mechanical and durability properties of cement-based materials containing waste recycled glass," *Journal of Cleaner Production*, vol. 198, pp. 891–906, 2018.

[15] A. Bentur, "Cementitious materials—nine millennia and A new century: past, present, and future," *Journal of Materials in Civil Engineering*, vol. 14, no. 1, pp. 2–22, 2002.

[16] G. S. Barger, M. R. Lukkarila, D. L. Martin et al., "Evaluation of a blended cement and a mineral admixture containing calcined clay natural pozzolans for high performance concrete," in *Proceedings of the 1997 International Purdue Conference on Concrete Pavement Design and Materials for High Performance, 6th, Indianapolis*, vol. 1, pp. 131–147, IEEE, Indianapolis, Indiana, USA, August 1997.

[17] M. F. Alnahhal, U. J. Alengaram, M. Z. Jumaat, F. Abutaha, M. A. Alqedra, and R. R. Nayaka, "Assessment on engineering properties and CO2 emissions of recycled aggregate concrete incorporating waste products as supplements to Portland cement," *Journal of Cleaner Production*, vol. 203, pp. 822–835, 2018.

[18] M. Fazilati and E. Mohammadi Golafshani, "Durability properties of concrete containing amorphous silicate tuff as a type of natural cementitious material," *Construction and Building Materials*, vol. 230, Article ID 117087, 2020.

[19] P. K. Mehta and P. J. Monteiro, *Concrete: Microstructure, Properties, and Materials*, McGraw-Hill Education, New York, 2014.

[20] P. Hewlett and M. Liska, Eds., *Lea's Chemistry of Cement and concrete*, Butterworth-Heinemann, Oxford, United Kingdom, 2019.

[21] B. Lothenbach, K. Scrivener, and R. D. Hooton, "Supplementary cementitious materials," *Cement and Concrete Research*, vol. 41, no. 12, pp. 1244–1256, 2011a.

[22] A. Goldman and A. Bentur, "The influence of microfillers on enhancement of concrete strength," *Cement and Concrete Research*, vol. 23, no. 4, pp. 962–972, 1993.

[23] S. C. Kou and C. S. Poon, "Properties of self-compacting concrete prepared with recycled glass aggregate," *Cement and Concrete Composites*, vol. 31, no. 2, pp. 107–113, 2009.

[24] U. A. Dogan and M. H. Ozkul, "The effect of cement type on long-term transport properties of self-compacting concretes," *Construction and Building Materials*, vol. 96, pp. 641–647, 2015.

[25] A. Mehta and D. K. Ashish, "Silica fume and waste glass in cement concrete production: a review," *Journal of Building Engineering*, vol. 29, Article ID 100888, 2020.

[26] R. Snellings, "Assessing, understanding and unlocking supplementary cementitious materials," *RILEM Technical Letters*, vol. 1, pp. 50–55, 2016.

[27] A. M. Rashad and D. M. Sadek, "An investigation on Portland cement replaced by high-volume GGBS pastes modified with micro-sized metakaolin subjected to elevated temperatures," *International Journal of Sustainable Built Environment*, vol. 6, no. 1, pp. 91–101, 2017.

[28] M. C. G. Juenger and R. Siddique, "Recent advances in understanding the role of supplementary cementitious materials in concrete," *Cement and Concrete Research*, vol. 78, pp. 71–80, 2015.

[29] A. M. Rashad, "Recycled waste glass as fine aggregate replacement in cementitious materials based on Portland cement," *Construction and Building Materials*, vol. 72, pp. 340–357, 2014.

[30] C. Shi and K. Zheng, "A review on the use of waste glasses in the production of cement and concrete," *Resources, Conservation and Recycling*, vol. 52, no. 2, pp. 234–247, 2007.

[31] A. Schmidt and W. H. F. Saia, "Alkali-aggregate reaction tests on glass used for exposed aggregate wall panel work," *ACI Materials Journal*, vol. 60, pp. 1235-1236, 1963.

[32] İB. Topçu and M. Canbaz, "Properties of concrete containing waste glass," *Cement and Concrete Research*, vol. 34, no. 2, pp. 267–274, 2004.

[33] S. Kozlova, K. Millrath, C. Meyer, and S. Shimanovich, "A suggested screening test for ASR in cement-bound composites containing glass aggregate based on autoclaving," *Cement and Concrete Composites*, vol. 26, no. 7, pp. 827–835, 2004.

[34] R. Oliveira, J. de Brito, and R. Veiga, "Incorporation of fine glass aggregates in renderings," *Construction and Building Materials*, vol. 44, pp. 329–341, 2013.

[35] G. S. Islam, M. H. Rahman, and N. Kazi, "Waste glass powder as partial replacement of cement for sustainable concrete practice," *International Journal of Sustainable Built Environment*, vol. 6, no. 1, pp. 37–44, 2017.

[36] Z. h He, P. m Zhan, S. g Du, B. j Liu, and W. b Yuan, "Creep behavior of concrete containing glass powder," *Composites Part B: Engineering*, vol. 166, pp. 13–20, 2019.

[37] D. Patel, R. P. Tiwari, R. Shrivastava, and R. K. Yadav, "Effective utilization of waste glass powder as the substitution of cement in making paste and mortar," *Construction and Building Materials*, vol. 199, pp. 406–415, 2019.

[38] K. I. M. Ibrahim, "Recycled waste glass powder as a partial replacement of cement in concrete containing silica fume and fly ash," *Case Studies in Construction Materials*, vol. 15, Article ID e00630, 2021.

[39] A. M. Rashad, "An investigation of high-volume fly ash concrete blended with slag subjected to elevated temperatures," *Journal of Cleaner Production*, vol. 93, pp. 47–55, 2015.

[40] H. Zhao, W. Sun, X. Wu, and B. Gao, "The properties of the self-compacting concrete with fly ash and ground granulated blast furnace slag mineral admixtures," *Journal of Cleaner Production*, vol. 95, pp. 66–74, 2015.

[41] H. Madani, M. N. Norouzifar, and J. Rostami, "The synergistic effect of pumice and silica fume on the durability and mechanical characteristics of eco-friendly concrete," *Construction and Building Materials*, vol. 174, pp. 356–368, 2018.

[42] E. Aprianti S, "A huge number of artificial waste material can be supplementary cementitious material (SCM) for concrete production – a review part II," *Journal of Cleaner Production*, vol. 142, pp. 4178–4194, 2017.

[43] M. Kooshafar and H. Madani, "An investigation on the influence of nano silica morphology on the characteristics of cement composites," *Journal of Building Engineering*, vol. 30, Article ID 101293, 2020.

[44] M. Sarıdemir, "Effect of silica fume and ground pumice on compressive strength and modulus of elasticity of high strength concrete," *Construction and Building Materials*, vol. 49, pp. 484–489, 2013.

[45] H. Toutanji, N. Delatte, S. Aggoun, R. Duval, and A. Danson, "Effect of supplementary cementitious materials on the compressive strength and durability of short-term cured concrete," *Cement and Concrete Research*, vol. 34, no. 2, pp. 311–319, 2004.

[46] H. Yazıcı, "The effect of silica fume and high-volume Class C fly ash on mechanical properties, chloride penetration and freeze–thaw resistance of self-compacting concrete," *Construction and Building Materials*, vol. 22, no. 4, pp. 456–462, 2008.

[47] A. Bagheri, H. Zanganeh, H. Alizadeh, M. Shakerinia, and M. A. S. Marian, "Comparing the performance of fine fly ash and silica fume in enhancing the properties of concretes containing fly ash," *Construction and Building Materials*, vol. 47, pp. 1402–1408, 2013.

[48] W. Wongkeo, P. Thongsanitgarn, A. Ngamjarurojana, and A. Chaipanich, "Compressive strength and chloride resistance of self-compacting concrete containing high level fly ash and silica fume," *Materials & Design*, vol. 64, pp. 261–269, 2014.

[49] Y. Li and A. K. H. Kwan, "Ternary blending of cement with fly ash microsphere and condensed silica fume to improve the performance of mortar," *Cement and Concrete Composites*, vol. 49, pp. 26–35, 2014.

[50] ASTM, *C1240-20: Standard Specification for Silica Fume Used in Cementitious Mixtures*, ASTM International, West Conshohocken, PA, USA, 2020a, https://www.astm.org/cgi-bin/resolver.cgi?C1240-20.

[51] ASTM, *C150/C150M-20: Standard Specification for Portland Cement*, ASTM International, West Conshohocken, PA, USA, 2020b, https://www.astm.org/cgi-bin/resolver.cgi?C150C150M-20.
[52] ASTM, *C989/C989M-18a: Standard Specification for Slag Cement for Use in Concrete and Mortars*, ASTM International, West Conshohocken, PA, USA, 2018b, https://www.astm.org/cgi-bin/resolver.cgi?C989C989M-18a.
[53] ASTM, *C1202-19: Standard Test Method for Electrical Indication of Concrete's Ability to Resist Chloride Ion Penetration*, ASTM International, West Conshohocken, PA, USA, 2019a, https://www.astm.org/cgi-bin/resolver.cgi?C1202-19.
[54] ASTM, *C127-15: Standard Test Method for Relative Density (Specific Gravity) and Absorption of Coarse Aggregate*, ASTM International, West Conshohocken, PA, USA, 2015a, https://www.astm.org/cgi-bin/resolver.cgi?C127-15.
[55] ASTM, *C128-15: Standard Test Method for Relative Density (Specific Gravity) and Absorption of Fine Aggregate*, ASTM International, West Conshohocken, PA, USA, 2015b, https://www.astm.org/cgi-bin/resolver.cgi?C128-15.
[56] ASTM, *C33/C33M-18: Standard Specification for Concrete Aggregates*, ASTM International, West Conshohocken, PA, USA, 2018a, https://www.astm.org/cgi-bin/resolver.cgi?C33C33M-18.
[57] ASTM, *C494/C494M-19: Standard Specification for Chemical Admixtures for Concrete*, ASTM International, West Conshohocken, PA, USA, 2019b, https://www.astm.org/cgi-bin/resolver.cgi?C494C494M-19.
[58] BSI, *EN 12390-2:2019. Testing Hardened concrete. Making and Curing Specimens for Strength Tests*, BSI, London, UK, 2019a.
[59] BSI, *EN 12390-3:2019. Testing hardened concrete. Compressive Strength of Test Specimens*, BSI, London, UK, 2019b.
[60] ASTM, *C496/C496M-17: Standard Test Method for Splitting Tensile Strength of Cylindrical Concrete Specimens*, ASTM International, West Conshohocken, PA, USA, 2017, https://www.astm.org/cgi-bin/resolver.cgi?C496C496M-17.
[61] ASTM, *C293/C293M-16: Standard Test Method for Flexural Strength of Concrete (Using Simple Beam with Center-Point Loading)*, ASTM International, West Conshohocken, PA, USA, 2016, https://www.astm.org/cgi-bin/resolver.cgi?C293C293M-16.
[62] V. Tanwar, K. Bisht, K. S. Ahmed Kabeer, and P. V. Ramana, "Experimental investigation of mechanical properties and resistance to acid and sulphate attack of GGBS based concrete mixes with beverage glass waste as fine aggregate," *Journal of Building Engineering*, vol. 41, Article ID 102372, 2021.
[63] D. Mostofinejad, S. M. Hosseini, F. Nosouhian, T. Ozbakkaloglu, and B. Nader Tehrani, "Durability of concrete containing recycled concrete coarse and fine aggregates and milled waste glass in magnesium sulfate environment," *Journal of Building Engineering*, vol. 29, Article ID 101182, 2020.
[64] A. Hendi, A. Behravan, D. Mostofinejad, H. Akhavan Kharazian, and A. Sedaghatdoost, "Performance of two types of concrete containing waste silica sources under MgSO4 attack evaluated by durability index," *Construction and Building Materials*, vol. 241, Article ID 118140, 2020.
[65] A. M. Diab, H. E. Elyamany, A. E. M. Abd Elmoaty, and M. M. Sreh, "Effect of nanomaterials additives on performance of concrete resistance against magnesium sulfate and acids," *Construction and Building Materials*, vol. 210, pp. 210–231, 2019.
[66] S. Singh, N. Nande, P. Bansal, and R. Nagar, "Experimental investigation of sustainable concrete made with granite industry by-product," *Journal of Materials in Civil Engineering*, vol. 29, no. 6, Article ID 04017017, 2017.
[67] D. Mostofinejad, F. Nosouhian, and H. Nazari-Monfared, "Influence of magnesium sulphate concentration on durability of concrete containing micro-silica, slag and limestone powder using durability index," *Construction and Building Materials*, vol. 117, pp. 107–120, 2016.
[68] D. K. Ashish, B. Singh, and S. K. Verma, "The effect of attack of chloride and sulphate on ground granulated blast furnace slag concrete," *Advances in Concrete Construction*, vol. 4, no. 2, pp. 107–121, 2016.
[69] P. Chindaprasirt, P. Paisitsrisawat, and U. Rattanasak, "Strength and resistance to sulfate and sulfuric acid of ground fluidized bed combustion fly ash–silica fume alkali-activated composite," *Advanced Powder Technology*, vol. 25, no. 3, pp. 1087–1093, 2014.
[70] A. M. Diab, A. E. M. Awad, H. E. Elyamany, and A. E. M. Abd Elmoaty, "Guidelines in compressive strength assessment of concrete modified with silica fume due to magnesium sulfate attack," *Construction and Building Materials*, vol. 36, pp. 311–318, 2012.
[71] E. Rozière, A. Loukili, R. El Hachem, and F. Grondin, "Durability of concrete exposed to leaching and external sulphate attacks," *Cement and Concrete Research*, vol. 39, no. 12, pp. 1188–1198, 2009.
[72] ASTM, *C267-01: Standard Test Methods for Chemical Resistance of Mortars, Grouts, and Monolithic Surfacings and Polymer Concretes*, ASTM International, West Conshohocken, PA, USA, 2012, https://www.astm.org/c0267-01.html.
[73] Aashto, *T 358-19: Standard Method of Test for Surface Resistivity Indication of Concrete's Ability to Resist Chloride Ion Penetration*, American Association of State Highway and Transportation Officials, Washington, D.C, 2019.
[74] ASTM, *C618-19: Standard Specification for Coal Fly Ash and Raw or Calcined Natural Pozzolan for Use in Concrete*, ASTM International, West Conshohocken, PA, USA, 2019c, https://www.astm.org/cgi-bin/resolver.cgi?C618-19.
[75] BSI, *BS 1881-122:2011. Testing concrete. Method for determination of water absorption*, BSI, London, UK, 2011.
[76] BSI, *EN 12390-8:2019. Testing Hardened concrete. Depth of Penetration of Water under Pressure*, BSI, London, UK, 2019c.
[77] R. Banar, P. Dashti, A. Zolfagharnasab, A. M. Ramezanianpour, and A. A. Ramezanianpour, "A comprehensive comparison between using silica fume in the forms of water slurry or blended cement in mortar/concrete," *Journal of Building Engineering*, vol. 46, Article ID 103802, 2022.
[78] O. Zaid, J. Ahmad, M. S. Siddique, F. Aslam, H. Alabduljabbar, and K. M. Khedher, "A step towards sustainable glass fiber reinforced concrete utilizing silica fume and waste coconut shell aggregate," *Scientific Reports*, vol. 11, no. 1, Article ID 12822, 2021.
[79] F. Ameri, P. Shoaei, N. Bahrami, M. Vaezi, and T. Ozbakkaloglu, "Optimum rice husk ash content and bacterial concentration in self-compacting concrete," *Construction and Building Materials*, vol. 222, pp. 796–813, 2019.
[80] S. A. Zareei, F. Ameri, P. Shoaei, and N. Bahrami, "Recycled ceramic waste high strength concrete containing wollastonite

particles and micro-silica: a comprehensive experimental study," *Construction and Building Materials*, vol. 201, pp. 11–32, 2019.

[81] R. Bani Ardalan, A. Joshaghani, and R. D. Hooton, "Workability retention and compressive strength of self-compacting concrete incorporating pumice powder and silica fume," *Construction and Building Materials*, vol. 134, pp. 116–122, 2017.

[82] S. A. Ghahari, A. M. Ramezanianpour, A. A. Ramezanianpour, and M. Esmaeili, "An accelerated test method of simultaneous carbonation and chloride ion ingress: durability of silica fume concrete in severe environments," *Advances in Materials Science and Engineering*, vol. 2016, pp. 1–12, Article ID 1650979, 2016.

[83] H. Madani, A. Bagheri, T. Parhizkar, and A. Raisghasemi, "Chloride penetration and electrical resistivity of concretes containing nanosilica hydrosols with different specific surface areas," *Cement and Concrete Composites*, vol. 53, pp. 18–24, 2014.

[84] N. Chahal, R. Siddique, and A. Rajor, "Influence of bacteria on the compressive strength, water absorption and rapid chloride permeability of concrete incorporating silica fume," *Construction and Building Materials*, vol. 37, pp. 645–651, 2012.

[85] K. Sakr, "Effects of silica fume and rice husk ash on the properties of heavy weight concrete," *Journal of Materials in Civil Engineering*, vol. 18, pp. 367–376, 2006.

[86] H. Du and K. H. Tan, "Properties of high volume glass powder concrete," *Cement and Concrete Composites*, vol. 75, pp. 22–29, 2017.

[87] J. Liu and D. Wang, "Influence of steel slag-silica fume composite mineral admixture on the properties of concrete," *Powder Technology*, vol. 320, pp. 230–238, 2017.

[88] F. Boukhelf, R. Cherif, A. Trabelsi, R. Belarbi, and M. Bachir Bouiadjra, "On the hygrothermal behavior of concrete containing glass powder and silica fume," *Journal of Cleaner Production*, vol. 318, Article ID 128647, 2021.

[89] K. Zheng, "Pozzolanic reaction of glass powder and its role in controlling alkali–silica reaction," *Cement and Concrete Composites*, vol. 67, pp. 30–38, 2016.

[90] B. Taha and G. Nounu, "Using Lithium Nitrate and Pozzolanic Glass Powder in concrete as ASR Suppressors," *Cement and Concrete Composites*, vol. 30, no. 6, pp. 497–505, 2008.

[91] B. Lothenbach, K. Scrivener, and R. D. Hooton, "Supplementary cementitious materials," *Cement and Concrete Research*, vol. 41, no. 12, pp. 1244–1256, 2011b.

[92] G. Chand, S. K. Happy, and S. Ram, "Assessment of the properties of sustainable concrete produced from quaternary blend of Portland cement, glass powder, metakaolin and silica fume," *Cleaner Engineering and Technology*, vol. 4, Article ID 100179, 2021.

[93] A. Pourjahanshahi and H. Madani, "Chloride diffusivity and mechanical performance of UHPC with hybrid fibers under heat treatment regime," *Materials Today Communications*, vol. 26, Article ID 102146, 2021.

[94] A. A. Aliabdo, A. E. M. Abd Elmoaty, and A. Y. Aboshama, "Utilization of waste glass powder in the production of cement and concrete," *Construction and Building Materials*, vol. 124, pp. 866–877, 2016.

[95] M. Mirzahosseini and K. A. Riding, "Influence of different particle sizes on reactivity of finely ground glass as supplementary cementitious material (SCM)," *Cement and Concrete Composites*, vol. 56, pp. 95–105, 2015.

[96] Q. Wang, P. Yan, J. Yang, and B. Zhang, "Influence of steel slag on mechanical properties and durability of concrete," *Construction and Building Materials*, vol. 47, pp. 1414–1420, 2013.

[97] S. Bhanja and B. Sengupta, "Influence of silica fume on the tensile strength of concrete," *Cement and Concrete Research*, vol. 35, no. 4, pp. 743–747, 2005.

[98] K. Bisht, K. S. A. Kabeer, and P. V. Ramana, "Gainful utilization of waste glass for production of sulphuric acid resistance concrete," *Construction and Building Materials*, vol. 235, Article ID 117486, 2020.

[99] R. Idir, M. Cyr, and A. Tagnit-Hamou, "Use of fine glass as ASR inhibitor in glass aggregate mortars," *Construction and Building Materials*, vol. 24, no. 7, pp. 1309–1312, 2010.

[100] T. Liu, S. Qin, D. Zou, and W. Song, "Experimental investigation on the durability performances of concrete using cathode ray tube glass as fine aggregate under chloride ion penetration or sulfate attack," *Construction and Building Materials*, vol. 163, pp. 634–642, 2018.

[101] J. Bijen, "Benefits of slag and fly ash," *Construction and Building Materials*, vol. 10, no. 5, pp. 309–314, 1996.

[102] G. Bye, P. Livesey, and L. Struble, *Portland Cement*, ICE Publishing, London, UK, 2011, https://www.icevirtuallibrary.com/doi/abs/10.1680/pc.36116.

[103] R. D. Hooton and J. J. Emery, "Sulfate resistance of a Canadian slag cement," *ACI Materials Journal*, vol. 87, pp. 547–555, 1990.

[104] R. S. Gollop and H. F. W. Taylor, "Microstructural and microanalytical studies of sulfate attack. V. Comparison of different slag blends," *Cement and Concrete Research*, vol. 26, no. 7, pp. 1029–1044, 1996a.

[105] R. S. Gollop and H. F. W. Taylor, "Microstructural and microanalytical studies of sulfate attack. IV. Reactions of a slag cement paste with sodium and magnesium sulfate solutions," *Cement and Concrete Research*, vol. 26, no. 7, pp. 1013–1028, 1996b.

[106] F. W. Locher, "The problem of the sulfate resistance of slag cements," *Zement-Kalk-Gibs*, pp. 9395–9401, 1966.

[107] D. D. Higgins, "Increased sulfate resistance of GGBS concrete in the presence of carbonate," *Cement and Concrete Composites*, vol. 25, no. 8, pp. 913–919, 2003.

[108] S. Ogawa, T. Nozaki, K. Yamada, H. Hirao, and R. D. Hooton, "Improvement on sulfate resistance of blended cement with high alumina slag," *Cement and Concrete Research*, vol. 42, no. 2, pp. 244–251, 2012.

[109] M. Whittaker and L. Black, "Current knowledge of external sulfate attack," *Advances in Cement Research*, vol. 27, no. 9, pp. 532–545, 2015.

[110] D. Bonen and M. D. Cohen, "Magnesium sulfate attack on portland cement paste — II. Chemical and mineralogical analyses," *Cement and Concrete Research*, vol. 22, no. 4, pp. 707–718, 1992.

[111] O. S. Baghabra Al-Amoudi, "Attack on plain and blended cements exposed to aggressive sulfate environments," *Cement and Concrete Composites*, vol. 24, no. 3-4, pp. 305–316, 2002.

[112] E. Ganjian and H. S. Pouya, "Effect of magnesium and sulfate ions on durability of silica fume blended mixes exposed to the seawater tidal zone," *Cement and Concrete Research*, vol. 35, no. 7, pp. 1332–1343, 2005.

[113] S. T. Lee, H. Y. Moon, and R. N. Swamy, "Sulfate attack and role of silica fume in resisting strength loss," *Cement and Concrete Composites*, vol. 27, no. 1, pp. 65–76, 2005.

[114] J. M. Ortega, M. D. Esteban, M. Williams, I. Sánchez, and M. Á Climent, "Short-term performance of sustainable silica fume mortars exposed to sulfate attack," *Sustainability*, vol. 10, no. 7, p. 2517, 2018.

[115] E. E. Hekal, E. Kishar, and H. Mostafa, "Magnesium sulfate attack on hardened blended cement pastes under different circumstances," *Cement and Concrete Research*, vol. 32, no. 9, pp. 1421–1427, 2002.

[116] K. Torii and M. Kawamura, "Effects of fly ash and silica fume on the resistance of mortar to sulfuric acid and sulfate attack," *Cement and Concrete Research*, vol. 24, no. 2, pp. 361–370, 1994.

[117] M. Y. Durgun and A. H. Sevinç, "Determination of the effectiveness of various mineral additives against sodium and magnesium sulfate attack in concrete by Taguchi method," *Journal of Building Engineering*, vol. 57, Article ID 104849, 2022.

[118] P. C. Hewlett and M. Liska, *Lea's Chemistry of Cement and Concrete*, Elsevier Science & Technology Books, Amsterdam, Netherlands, 2017.

[119] M. Alexander, A. Bertron, and N. De Belie, "Performance of cement-based materials in aggressive aqueous environments: state-of-the-art report," *RILEM TC 211 - PAE*, Springer Dordrecht, , vol. Volume 10, p. 464, 2013.

[120] K. L. Jain, G. Sancheti, and L. K. Gupta, "Durability performance of waste granite and glass powder added concrete," *Construction and Building Materials*, vol. 252, Article ID 119075, 2020.

[121] P. Sturm, G. J. G. Gluth, C. Jäger, H. J. H. Brouwers, and H. C. Kühne, "Sulfuric acid resistance of one-part alkali-activated mortars," *Cement and Concrete Research*, vol. 109, pp. 54–63, 2018.

[122] Y. Senhadji, G. Escadeillas, M. Mouli, H. Khelafi, and Benosman, "Influence of natural pozzolan, silica fume and limestone fine on strength, acid resistance and microstructure of mortar," *Powder Technology*, vol. 254, pp. 314–323, 2014.

[123] A. Hendi, A. Behravan, D. Mostofinejad, S. M. Moshtaghi, and K. Rezayi, "Implementing ANN to minimize sewage systems concrete corrosion with glass beads substitution," *Construction and Building Materials*, vol. 138, pp. 441–454, 2017.

[124] M. T. Bassuoni and M. L. Nehdi, "Resistance of self-consolidating concrete to sulfuric acid attack with consecutive pH reduction," *Cement and Concrete Research*, vol. 37, no. 7, pp. 1070–1084, 2007.

[125] Z.-T. Chang, X.-J. Song, R. Munn, and M. Marosszeky, "Using limestone aggregates and different cements for enhancing resistance of concrete to sulphuric acid attack," *Cement and Concrete Research*, vol. 35, no. 8, pp. 1486–1494, 2005.

[126] N. De Belie, H. J. Verselder, B. De Blaere, D. Van Nieuwenburg, and R. Verschoore, "Influence of the cement type on the resistance of concrete to feed acids," *Cement and Concrete Research*, vol. 26, no. 11, pp. 1717–1725, 1996.

[127] A. Pilvar, A. A. Ramezanianpour, H. Rajaie, and S. M. M. Karein, "Practical evaluation of rapid tests for assessing the Chloride resistance of concretes containing Silica Fume," *Computers and Concrete*, vol. 18, no. 6, pp. 793–806, 2016.

[128] M. Delnavaz, A. Sahraei, A. Delnavaz, R. Farokhzad, Sh Amiri, and S. Bozorgmehrnia, "Production of concrete using reclaimed water from a ready-mix concrete batching plant: life cycle assessment (LCA), mechanical and durability properties," *Journal of Building Engineering*, vol. 45, Article ID 103560, 2022.

[129] S. M. Motahari Karein, A. A. Ramezanianpour, T. Ebadi, S. Isapour, and M. Karakouzian, "A new approach for application of silica fume in concrete: wet granulation," *Construction and Building Materials*, vol. 157, pp. 573–581, 2017.

[130] J. M. R. Dotto, A. G. Abreu, D. C. C. Dal Molin, and I. L. Müller, "Influence of silica fume addition on concretes physical properties and on corrosion behaviour of reinforcement bars," *Cement and Concrete Composites*, vol. 26, no. 1, pp. 31–39, 2004.

[131] C. Naito, J. Fox, P. Bocchini, and M. Khazaali, "Chloride migration characteristics and reliability of reinforced concrete highway structures in Pennsylvania," *Construction and Building Materials*, vol. 231, Article ID 117045, 2020.

[132] K. Gowers and S. Millard, "Measurement of concrete resistivity for assessment of corrosion," *ACI Materials Journal*, vol. 96, pp. 536–541, 1999.

[133] R. B. C. Sales, F. A. Sales, E. P. Figueiredo, W. J. dos Santos, N. D. S. Mohallem, and M. T. P. Aguilar, "Durability of mortar made with fine glass powdered particles," *Advances in Materials Science and Engineering*, vol. 2017, pp. 1–9, 2017.

[134] O. Kayali, M. S. H. Khan, and M. Sharfuddin Ahmed, "The role of hydrotalcite in chloride binding and corrosion protection in concretes with ground granulated blast furnace slag," *Cement and Concrete Composites*, vol. 34, no. 8, pp. 936–945, 2012.

[135] K. Y. Yeau and E. K. Kim, "An experimental study on corrosion resistance of concrete with ground granulate blast-furnace slag," *Cement and Concrete Research*, vol. 35, no. 7, pp. 1391–1399, 2005.

[136] J. A. Jain and N. Neithalath, "Chloride transport in fly ash and glass powder modified concretes – influence of test methods on microstructure," *Cement and Concrete Composites*, vol. 32, no. 2, pp. 148–156, 2010.

[137] H. Madani, A. Bagheri, and T. Parhizkar, "The pozzolanic reactivity of monodispersed nanosilica hydrosols and their influence on the hydration characteristics of Portland cement," *Cement and Concrete Research*, vol. 42, no. 12, pp. 1563–1570, 2012.

[138] G. Singh and R. Siddique, "Effect of iron slag as partial replacement of fine aggregates on the durability characteristics of self-compacting concrete," *Construction and Building Materials*, vol. 128, pp. 88–95, 2016.

[139] S. Gupta, H. W. Kua, and S. D. Pang, "Effect of biochar on mechanical and permeability properties of concrete exposed to elevated temperature," *Construction and Building Materials*, vol. 234, Article ID 117338, 2020.

[140] A. Khaloo, M. Mohammadhasani, and K. Faghihi, "Experimental investigation of eco-friendly concrete utilising waste glass," *Proceedings of the Institution of Civil Engineers - Engineering Sustainability*, vol. 173, no. 4, pp. 174–183, 2020.

[141] F. A. Sabet, N. A. Libre, and M. Shekarchi, "Mechanical and durability properties of self consolidating high performance concrete incorporating natural zeolite, silica fume and fly ash," *Construction and Building Materials*, vol. 44, pp. 175–184, 2013.

[142] CEB–FIP, "Diagnosis and Assessment of concrete Structures – State of Art Report, CEB Bulletin 192," pp. 83–85, Euro-International Concrete Committee (Comité Euro-International du Béton), 1989.

[143] M. S. Shetty and A. K. Jain, *Concrete Technology (Theory and Practice)*, S.Chand and Company Limited, New Delhi, India, 2019.

[144] F. Bernard and S. Kamali-Bernard, "Performance simulation and quantitative analysis of cement-based materials subjected to leaching," *Computational Materials Science*, vol. 50, no. 1, pp. 218–226, 2010.

[145] K. Samimi, S. Kamali-Bernard, A. Akbar Maghsoudi, M. Maghsoudi, and H. Siad, "Influence of pumice and zeolite on compressive strength, transport properties and resistance to chloride penetration of high strength self-compacting concretes," *Construction and Building Materials*, vol. 151, pp. 292–311, 2017.

[146] K. K. Aligizaki, *Pore Structure of Cement-Based Materials: Testing, Interpretation and Requirements*, CRC Press, Boca Raton, Florida, United States, 2004.

[147] S. Mindess, F. Young, and D. Darwin, *ConcreteTechnical Documents*, p. 585, Springer, Berlin, Germany, 2003.

[148] S. Ahmad, O. S. Baghabra Al-Amoudi, S. M. S. Khan, and M. Maslehuddin, "Effect of silica fume inclusion on the strength, shrinkage and durability characteristics of natural pozzolan-based cement concrete," *Case Studies in Construction Materials*, vol. 17, Article ID e01255, 2022.

[149] C. Ince, A. Hamza, S. Derogar, and R. J. Ball, "Utilisation of waste marble dust for improved durability and cost efficiency of pozzolanic concrete," *Journal of Cleaner Production*, vol. 270, Article ID 122213, 2020.

[150] S. Moradi and S. Shahnoori, "Eco-friendly mix for Roller-Compacted Concrete: effects of Persian-Gulf-Dredged marine sand on durability and resistance parameters of concrete," *Construction and Building Materials*, vol. 281, Article ID 122555, 2021.

[151] P. A. M. Basheer, P. R. V. Gilleece, A. E. Long, and W. J. Mc Carter, "Monitoring electrical resistance of concretes containing alternative cementitious materials to assess their resistance to chloride penetration," *Cement and Concrete Composites*, vol. 24, no. 5, pp. 437–449, 2002.

[152] V. S. Ramachandran and J. J. Beaudoin, *Handbook of Analytical Techniques in Concrete Science and Technology: Principles, Techniques, and Applications*, p. 1003, Elsevier Science, Amsterdam, Netherlands, 2000.